An Investigation of Electronic Properties in Oxide and sulphide Nanoclusters in Dielectric Background.

THESIS RE-SUBMITTED FOR THE DEGREE OF
DOCTOR OF PHILOSOPHY (SCIENCE)
OF

JADAVPUR UNIVERSITY

By

Moumita Barman

BIJOY KRISHNA GIRLS' COLLEGE
HOWRAH 711 101
WEST BENGAL, INDIA

FEBRUARY 2017

CERTIFICATE FROM THE SUPERVISORS

This is to certify that the thesis entitled "**An Investigation of Electronic Properties in Oxide and sulphide Nanoclusters in Dielectric Background**" re-submitted by **Moumita Barman** who got his name registered on 08 / 01 / 2008 for the award of **Ph.D. (Science) degree** of **Jadavpur University**, is absolutely based upon his own work under the supervision of Dr. Aloke Kr. Sarkar and Prof. Tapas Ranjan Middya and neither this thesis nor any part of it has been re-submitted for any degree / diploma or any other academic award anywhere before.

(Signature fo the Supervisors & date with official seal)

1. Aloke Kumar Sarkar 17.2.17

Dr. Aloke Kumar Sarkar
Associate Professor, Physics (Retd.)
Bijoy Krishna Girls' College
5/3, M. G. Road, Howrah-711 101

2. Tapas Ranjan Middya 17/2/17

Tapas Ranjan Middya
Professor
Department of Physics
Jadavpur University
Kolkata-700032

ACKNOWLEDGEMENTS

My respected supervisors, Dr. Aloke Kr. Sarkar, Reader, Dept. of Physics, B.K. Girls' College, Howrah and Prof. Tapas Ranjan Middya, Professor, Dept. of Physics, Jadavpur Univ. Kolkata, guided me by their constructive suggestion and encouragement and spearheaded the research activity by their constant directive.

My colleagues, Mr Partha Krishna Ghosh, Mr. Arup Dutta, and Mr. Somnath paul have extended their co-operation and technical assistance in an uncounted number of ways.

I wish to thank Department of Physics, B.K. Girls' College where I completed this work and I acknowledge the cooperation of the departmental members at various stages.

Inter University Consortium for Department of Atomic Energy Facilities (IUC-DAEF), Indore, and SAIF Mumbai, India are acknowledged for extending their laboratory facilities.

I also wish to extend my acknowledgement to my relatives and friends who shared different moments at different situations.

My loving parents and sister whose continuous support, encouragement and love through all my life helped me to concentrate in study and research work.

I want to give thank my husband Sourav for continuous help in different part of life, and to complete the work.

Finally I want to give my warm gratitude from my heart to my guide Dr. Aloke Kumar Sarkar to being a guide in true sence in all part of life.

Preface

In recent years the whole idea of nano science and nano-technology has become most important and exciting forefront due to their unique, fascinating properties in the field of physics, chemistry, engineering and biology. Nano science occurs at the intersection of traditional science and engineering, quantum mechanics and the most basic process of life itself. The nature of the quantum confinement of charge in such a system provides an unique opportunities of study both from both science and technological view point. Modification in the density of state (DOS) function the system exhibits unique electronic and related properties. Nanotechnology is based on the recognition that particles less than size of 100 nm (a nanometer is a billionth of a meter) impart to nanostructure built from them new properties and behavior. So for the example the electronic structure, conductivity, reactivity, melting temperature and mechanical properties through low dimensional nano-complex has developed considerable interest in special types of nano-science device.

In this present research synthesis of nano- structures are to be realized by natural self assembly of different nano-structures (namely oxides and sulphides of some d and f band metallic elements- wide band semiconductors e. g. ZnO, ns, CuO, CuS, TiO MoS, NiS etc) in strong dielectric / firm capping background. The electronic properties of the developed specimen are to be probed using spectro-photometric, Impedance spectroscopy, Photoluminescence, Electroluminescence and DC volt ampere with temperature variation set up. The electronic properties of the specimen suffer change with the variation of doping concentration. The wide bandgap semiconductors have revealed the new area of interest such as dilute magnetic semiconductor (DMS) property of them.

In chapter 1 I have briefly discussed the oxide and sulphide conductors and their physical aspects. In chapter 2 an attempt has been made to find the magnetic behavior of NiS thin film. It also discussed the potential application of it. Chapter 3 discussed the work done on ZnS nano-clusters. Chapter 4 and 5 discussed on studies undertaken the optical and electrical property on NiO and ZnO. Here I have reported studies carried out on the magnetic nature of doped ZnO. Variation of doping level changes the magnetic nature of the specimen. In chapter 6 reported the result of investigation the change in magnetic nature as well as electronic property due to variation of the doping concentration in CoO nano sample.

Objectives

It has been observed that oxides and sulphides of 4d and 5d transition metal exhibit novel phenomena in regard of structural, physical and chemical properties which are of great fundamental and technological importance The strong influence of the quantum spin-orbit interaction and orbital order in 4d- and 5d- materials are responsible for the mentioned properties. The objective of this thesis is present a comprehensive report on outcome of the investigation of electronic properties in developed oxide and sulphide nanoclusters in dielectric background. These studies include work on III-V Oxides of TM and developed systems with VIII and II-VI metallic composites as DMS materials. In these studies Mn and Gd are used as spin manipulative dopant. This work also makes an attempt to investigate the magnetic characteristics of some developed sulphides and doped Oxides.

Significance of the study

The research field on dilute magnetic semiconductors (DMS) [1, 2] is one of the important field.. These oxides/sulphides of TM along with suitable dopant are of great interest because of the novelty of their fundamental properties and also due to their potential as the future semiconductor technologies which promise integration of magnetic, semi conducting and optical properties and a combination of information processing and storage functionalities. They should be compatible with existing microelectronic technologies and have potential as low-dissipation, non-volatile, and nano-scale alternatives to present day microelectronics. This work involves chemical/ electrochemical sol-gel technique for growth of mentioned materials, characterization, and studies on their electrical transport and optical properties. Some .new results obtained from the present study may contribute a good knowledge in the art of this field.

References:

1. Nanomagnetism and spintronics ,Fabrication, Materials, Characterization and Applications- F. Nasirpuri & A Nogaret (eds), World Scientific, Singapore,2011
2. Theory of ferromagnetic (III, Mn)V semiconductors, Jungwirth et al, Rev. Mod. Phys. 78, 809 (2006)

List of publications

1. Electrical Noise in Sol-Gel synthesized ZnO Nanocluster dispersed polymer. Moumita Barman, S.S. Pradhan and A. Sarkar, DAE Solid State Physics, Proc. 51, 2006, pp 265.
2. Characteristics of ZnS nano- dispersed Polymer. Moumita Barman and A. Sarkar, DAE Solid State Physics, Proc. 50, 2007,pp 175.
3. A study on confined ZnS Nano-clusters in polymeric background. Moumita Barman, S. S. Pradhan and A. Sarkar, DAE Solid State Physics, Proc. 52, 2007,pp186.
4. A study on NiS Nano-clusters. Moumita Barman, S.S Pradhan and A. Sarkar. DAE Solid State Physics, Proc. 53,2008, pp 349-350.
5. Electronic Properties in Mn Doped and Pure NiO clusters. Moumita Barman, Somnath Paul and A. Sarkar, AIP Conf. Proc. 1536, 2013, pp427-428.
6. A study of magnetic properties in confined soi-gel synthesized NiS nano-clusters. Moumita Barman, Somnath Paul and A. Sarkar. Adv. Appl.Sci. Res., 4(5) 2013, pp343-349.
7. Bulk and Surface Electronic Properties in synthesized CoO clusters. Moumita Barman, Somnath Paul and A. Sarkar, Int. J.Engg.Res. Tech, AMRP Conf. Proc., 2013.
8. Infrared absorption of Nickel Sulphide complex of Gum Arabica. S.S.Pradhan, Moumita Barman and A. Sarkar, I.N.T.J.Engg.Res. Tech, AMRP Conf. Proc., 2013,pp 89-90.
9. Electronic and Optical Character of Cobalt Doped Zinc Oxide. Moumita Barman, Somnath Paul and A. Sarkar, Adv. Appl.Sci. Res., 5(1) 2014, pp 311-315.
10. Optical Aspects of Cobalt doped nano Zinc Oxide. Moumita Barman, Somnath Paul and A. Sarkar, Tech.Lett., 1(10) 2014,pp 13-15.

Contents

Chapter-6 Bulk and Surface Electronic Properties in synthesized CoO clusters.

LIST OF FIGURES.

Chapter-1.

Oxides and sulphides of metals.

1.1 Introduction.

1.1.1 What are basic conductors?

Conductor is a type of material which permits the flow of electric charges through it. Conducting materials include metals, electrolytes, superconductors, plasmas and some nonmetallic conductors such as graphite and Conductive polymers. All conductors contain electrical charges, which move when an electric potential difference is applied across it. This flow of charge is leads to an electric current in it. In most materials, the direct current is proportional to the voltage (as determined by Ohm's law), provided the temperature remains constant and the material remains in the same shape and state.

1.1.2 Nano complex conductor

Recently a dramatic change was observed in electrical properties of quantum sized nano-complex system over its bulk counterpart. The word nano means very small i.e. objects having dimension in nanometer scale, scientifically defined as atoms or molecule bonded in a cluster with a dimension of less than 100 nm. Nano-structures have attracted steadily growing interest due to their unique, fascinating properties as well as their possible role in the new types of application to nano-scale device in contrast to the bulk materials. The nature of the quantum confinement of charge in such a system provides a unique opportunity of study both from science and technological view point. Modification in the density of state (DOS) function the system exhibits unique electronic and related properties. The electrical transport through low dimensional nano-complex has been developed considerable interest in utilizing their intrinsic properties to exploit a possible role in special types of nano-scale device. In this thesis synthesis of nano- structures are to be realized by natural self assembly of constituent atoms/ molecules. Different nano-structures (namely oxides and sulphides of some d and f band metallic elements- wide band semiconductors e. g. ZnO, ZnS, CuO, CuS, TiO MoS, NiS etc) are developed in

dielectric or firm capping background. The self assembly is to be exploited following a bottom-up *in -situ* process followed by sol-gel process. The developed clusters are supposed to occupy some localized position in the background medium and provide additional localized energy levels for the charge carriers.

1.1.3 Oxide conductor

Conducting oxides (M_yO_x) metal oxides having good optical property and high electrical conductivity are of interest in this study. Most of the conducting oxides (CO) are binary or ternary compounds containing one or two metallic elements. The resistivity of the conducting oxides may be as low as ~10^{-4} ohm-cm or less. This important combination of conductivity and transparency is usually difficult to achieve in intrinsic or pure oxides. For obtaining high conductivity in the materials, either they have to be non-stoichiometric in composition or should be doped with appropriate element/ compound. Controlled doping of transition metal ions in these oxides is desirable such that an enhanced electrical conductivity without degrading their optical properties may be obtained. Some oxide semiconductors are extensively used for transparent electrodes. The different oxide semiconductors those paid attention in this thesis are ZnO, CoO, NiO and their doped version. CO with wide band gap, transparent, high carrier density, cost effective and can be grown in polymers have wide range of application potential. It has been found that some oxide semiconductors can be used as host compounds for magnetic semiconductors. Oxide semiconductors of the type ZnO and doped ZnO are ubiquitous in electronics as transparent conducting electrodes.

1.1.4 Sulphide conductor

The metal sulphides exhibit a great diversity of electrical and magnetic properties with both scientific interest and practical applications. These properties offer major constraint in the study of models of the electronic structure in sulphides. The pure and doped systems of certain sulphides have good application potential in the electronics industry (optical devices, photovoltaic, photodiode and magnetic recording devices). Metallic sulphides are also components of many thin film devices and have been extensively investigated as part of the nano-technology revolution. Certain electrical and magnetic properties of sulphide minerals contribute to

geomagnetism and paleo-magnetism, and provide geophysical prospector with exploration tool for metallicferous ore deposits.

1.2 Application potential of Sulphide conductors.

There are many potential application of this type of material some of most fascinating uses are listed below

a) Transparent electrode for flat panel displays.
b) Transparent electrode for photovoltaic cells.
c) Low emissivity windows.
d) Thin film transistors.
e) Light emitting diodes.
f) Semiconductor lasers.

1.3 Electronic properties of Sulphide conductors.

This present research likes to devise an electrical method of characterizing a nano-system by the following root. The inclusion of nano-meter scale material in background host exhibits electrical properties manifesting quantum confinement effects and strong electrical non-linearity with apparent appearance of electrical noise. The nano-scale pattern formation has yield interesting results besides the size controlling the parameter of nano-clusters while its preparation. The preliminary results of d.c. I-V characteristics shows that the very existence of 1/f type noise is due to the presence of many activated centre in the form of nano- clusters in the specimen. The distribution of fluctuations in the d.c I-V characteristics is due to the transition between two states in the composite. The observed conductance fluctuations are thus a finger print or marked characteristics of the existence of nano-cluster type impurities in configured specimen. In these real experimental results the observed noise appeared as an admixture of Nyquist/Johnson, shot noise and 1/f types of noise originating mostly from the quantum confinement of 3D nano-cluster in the specimen.

1.4 Optical and semi-conducting aspects of Sulphide conductors.

The optical properties of solids are largely dependent on electronic polarizability of ions, which is the fall out of deformation of their electronic clouds under application of an external electromagnetic field. The phenomenon leads to many

interesting optical properties of materials such as refraction, electro-optical effect and other nonlinear optical aspects. The various aspects of polarization of ions in different crystalline and amorphous materials are of considerable interest [1]. A quantitative estimate of the electronic polarizability of ions in simple oxides [2] and oxide glasses has gained new momentum. The polarizability approach is found to be important to design optical functional materials and to search for novel glasses with higher optical performances such as oxide glasses with high second- and third order optical nonlinearity.

Band gap, in a solid is a forbidden energy zone where no electronic states are allowed. In practice a quantum of energy is required to promote an electron from the top of the valence band and the bottom of the conduction band in insulators and semiconductors. In a solid band gap is an important factor that some how determines the electrical conduction in a solid. Solids having large band gaps are called insulators, and that with smaller band gaps are popular semiconductors. Conducting solids may have very small band gaps or no band gap due to band overlap. The mentioned band gap is often known as electric or transport band gap. In solid it is the threshold energy for creating charge separation i.e. an electron–hole pair leading to electrical transport. The optical band gap in a solid is however, the threshold energy for photons to be absorbed to produce bound electron-hole pair. In general for organic or oxide solids transport or electrical band gap is greater in magnitude than that of optical band gap. However for conventional semiconductors the band gaps are practically same.

Magnetic Properties of Oxides

Following “TOPICAL REVIEW — Magnetism, magnetic materials and interdisciplinary research “[3] oxides are the candidates for magnetic semiconductors and oxide materials have a long drawn research history. The oldest of functional oxides are permanent magnets of lodestone consisting of Fe_3O_4 which were used as directional compasses in ancient world, Twentieth century research finds, ferromagnetic oxide nano-particles (Fe_2O_3 and later CrO_2)as materials in recording media in magnetic tapes. Ferroelectric oxides were also provides a major research field in material science. The journey started with the first observation of electric hysteresis in Rochelle salt. In 1985, a major breakthrough was recorded in

superconductivity. It has been found that superconducting oxides exhibits superconductivity at 35 K in the La–Ba–Cu–O system-known as high T_c material [4] The "colossal magneto-resistance" (CMR) and complex phase transitions are observed in mixed valence manganites which have been intensively explored subsequently.[5] These materials are known that in CMR materials, the esteemed physical properties in the materials are dominated by the "double exchange" interactions and Jahn–Teller distortions as a result of the complicated interactions between electronic, magnetic, and structural degrees of freedom. The metallic binary oxides like Fe_3O_4, CrO_2, and EuO are also potential candidates because of their high spin polarization ratio (~100%). Recently it has been found that, multiferroic oxides (BiFeO, $BaTiO_3$, $TbMnO_3$, etc.) with more than two ferroic orders have become a rapid growing research field. In general wide band gap materials are insulating, however, conducting materials are opaque to electro-magnetic radiation at visible wavelengths. The wide band gap oxides semiconductors like ZnO, TiO_2, In2O_3, etc. are unique since they may be good conductors due to the presence of inherent defects while simultaneously being transparent in the visible region.[6] Hence, wide band gap oxides based on diluted magnetic oxides, like ZnO, TiO_2, In_2O_3, SnO_2 are promising oxide candidates for spintronics applications. Apart from the pure oxides doped variety of ZnO, $(In,Sn)_2O_3$ (ITO) doped with different transition metals (Co, Mn, Fe, Cu,Ni, V, etc.) and non-magnetic (N, H, etc.) dopants, occupied a rapid growing research field. Moreover, the magnetic properties of wide band gap oxides span from diamagnetic, paramagnetic to ferromagnetic and antiferromagnetic, and their chemical reactivity can be tailored from being highly reactive to inert. The mentioned amazing properties originate from the strong and competitive exchange coupling between charge, orbital, lattices, and spin effects in these oxide materials. [7]

Magnetoresistant

Magneto resistance is phenomena where value of electrical resistance of a material to changes under the application of an external magnetic field on it. This is also known as ordinary magneto resistance (OMR) and is given by,

$$\delta_H = \frac{R(0) - R(H)}{R(H)}$$

R(0) is the no field electrical resistance of a specimen, R(H) is that under application of external field H.

Recently it has been observed that some materials and multilayer exhibit magneto resistance different from OMR type namely giant magneto resistance (GMR), colossal magneto resistance (CMR) and tunnel magneto resistance (TMR).

Giant magneto resistance (GMR) [8,9] is a quantum mechanical phenomena at macroscopic scale .The type of magneto resistance observed in structures consisting alternate thin-films of ferromagnetic and non-magnetic conducting layers.

In this phenomena a significant change in the electrical resistance, of a specimen is observed, depending on the nature of magnetization of adjacent ferromagnetic layers are in a parallel or an antiparallel to electric field alignment. The resistance is low for parallel alignment compared to that in antiparallel alignment.

Colossal magneto resistance (CMR) is a property in which change in t electrical resistance in presence of a magnetic field of typical materials, are observed to be very high compared to that in OMR. The effect best observed in Manganese based mixed-valence materials in perovskite structure [10]. A complete understanding that can quantify of the CMR is still a subject of research.

Tunnel magneto resistance (TMR) [11] is a type of magneto-resistive effect found to be observed in a magnetic tunnel junction (MTJ), which consists of two ferromagnets separated by a thin insulator. When an insulating layer is very thin enough (~ nanometers), electrons can tunnel through from one ferromagnet into the other. This process is not allowed in classical Physics; hence the TMR is a quantum phenomenon.

1.5 Measurement techniques.

1.5.1 Electrical conduction.

1.5.1.1 Ampere-Volt Characteristics

Study of Ampere-Volt (I-V) characteristics of a material is important in regard of electronic conduction in it. The nature of I-V characteristics provides information of electronic and ‘hole’ contribution to the total electronic conductivity.

The electronic conductivity is due to negative electrons and positive “holes” is given by,

$$\sigma_{electron} = \sigma_e + \sigma_h \quad (1.1)$$

The ionic conductivity is due to cation and anion species of the material. Cationic transference number

$$\tau_+ = (\sigma_+ / \sigma_{ion}) \quad (1.2)$$

The anionic transference number

$$\tau_- = 1 - \tau_+. \quad (1.3)$$

1.5.1.2 Impedance Spectroscopy.

Impedance spectroscopy can play an important role in fundamental and applied electro-chemistry and material science in the coming years. It is the method of choice for characterizing the electrical behavior of systems in which the overall system response is measured by strongly coupled processes. Nowadays high quality impedance bridges and automatic measuring instrument can measure the complex electro-impedance between milihertz to megahertz of frequency range. It is a powerful method of characterizing many of the electrical of materials and their interfaces with electronically conducting electrodes. It may be used to investigate the dynamics of bound or mobile charge in the bulk or interfacial regions of any kind of solid/liquid material, ionic semiconducting, mixed conductor (elecronic+ionic) and even insulators (dielectric).

Basic impedance spectroscopy experiment

Electrical measurements to evaluate the electro-chemical behavior of electrode and/or electrolyte materials are usually made with proto-cell containing an experimental sample sandwiched between two identical polished electrodes in the form of a circular cylinder or rectangular parallelepiped shape. The general approach is to apply an a.c. electrical stimulus (a known voltage or current) to the electrodes such that the specimen may be at near equilibrium state and observed response (the resulting current or voltage, phase angle and impedance) recorded.

1.5.1.3 Impedance Plot

The plot is a popular format for evaluating impedance data, is the Nyquist plot. This format is also known as Cole-Cole plot or a Complex Impedance plot. The imaginary impedance component Z'' is plotted against real impedance component Z' at each excitation frequency.

1.5.2 Optical absorption.

Basic principle of spectrophotometer

The first assumption in spectroscopic measurements is the Beers law, relationship applies between a change in spectrometer response and the concentration of analyze material present in a sample specimen. The Bouguer, Lambert and Beer relationship assumes that the transmission of a sample with in an incident beam is equivalent to 10 exponent the negative product of the molar extinction coefficient (in L /mol.cm), multiplied by the concentration of a molecule in solution times the path length (in cm) of the sample in solution. So Beers relationship is

$$T=I/I_0= 10^{-ecl} \quad (1.4)$$

T is the transmittance, I_0 is the intensity of incident energy, where I is the intensity of transmitted light, e is the molar extinction coefficient, c is the concentration and l is the path length. To simplify the equation in more standard form showing absorbance as a logarithmic term used to linearize the relationship between the spectrophotometer response and concentration, gives the following expressions as the relationship between absorbance and concentration.

$$\text{Absobance , } A= -\log(I/I_0)=-\log(T)=ecl \quad (1.5)$$

The goal in the design of an optical spectrometer is to maximize the energy (or radiant power) from a light source through the spectrometer to the detector. The optical throughput for a spectrometer is dependent on multiple factors, such as the

light source area the apertures present within the light path lens transmittance and the mirror reflectance losses, the exit aperture and the detector efficiency.

UV-VIS Spectrophotometer

The ultraviolet-visible (UV-VIS) spectrophotometer is an instrument commonly used in the laboratory that analyzes compounds in ultraviolet and visible region of the electromagnetic spectrum. Generally UV-VIS spectroscopy looks at electronic transition while infrared spectroscopy looks at vibrational motion in the material. It determines the wavelength and maximum absorbance of compounds.

Many molecules absorb ultraviolet or visible light. The absorbance of a solution increases as attenuation of the beam increases. Different molecules absorb radiation of different wavelengths. An absorption spectrum will show a number of absorption bands corresponding to structural groups within the molecule. For example, the absorption that is observed in the UV region for the carbonyl group in acetone is of the same wavelength as the absorption from the carbonyl group in diethyl ketone.

A molecule of any substance has an internal energy which can be considered as the sum of the energy of its electrons, the energy of vibration between its constituent atoms and the energy associated with rotation of the molecule. The electronic energy levels of simple molecules are widely separated and usually only the absorption of a high energy photon, that is one of very short wavelength, can excite a molecule from one level to another. In complex molecules the energy levels are more closely spaced and photons of near ultraviolet and visible light can effect the transition. These substances, therefore, will absorb light in some areas of the near ultraviolet and visible regions. The vibrational energy states of the various parts of a molecule are much closer together than the electronic energy levels and thus protons of lower energy (longer wavelength) are sufficient to bring about vibrational changes. Light absorption due to only to vibrational changes occurs in the infrared region. The rotational energy states of molecules are so closely spaced that light in the far infrared and microwave regions of the electromagnetic spectrum has enough energy to cause these small changes.

For ultraviolet and visible wavelengths, absorption spectrum of a molecule (i.e., a plot of its degree of absorption against the wavelength of the incident radiation) should show a few very sharp lines. Each line should occur at a wavelength where the energy of an incident photon exactly matches the energy required to excite an electronic transition. In practice it is found that the ultraviolet and visible spectrum of most molecules consists of a few humps rather than sharp lines. These humps show that the molecule is absorbing radiation over a band of wavelengths. One reason for this band, rather than line absorption is that an electronic level transition is usually accompanied by a simultaneous change between the more numerous vibrational levels. Thus, a photon with a little too much or too little energy to be accepted by the molecule for a 'pure' electronic transition can be utilized for a transition between one of the vibrational levels associated with the lower electronic state to one of the vibrational levels of a higher electronic state. The energy levels of a molecule shown in fig 1.1.

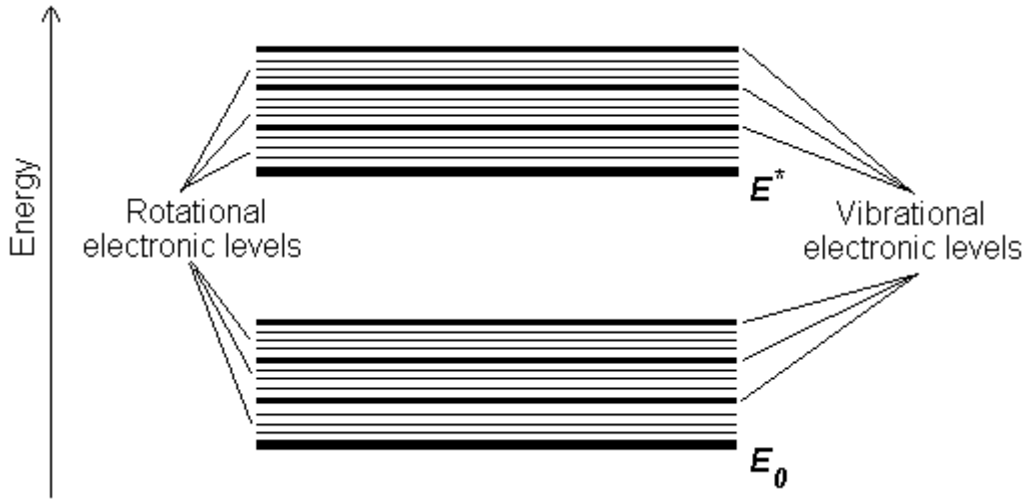

Fig 1.1: Energy levels of a molecule.

A molecule or ion will exhibit absorption in the visible or ultraviolet region when radiation causes an electronic transition within its structure. Thus, the absorption of light by a sample in the ultraviolet or visible region is accompanied by a change in the electronic state of the molecules in the sample. The energy supplied by the light will promote an electron from their ground state orbitals to higher energy

excited state orbitals or anti-bonding orbitals. Potentially, three types of ground state orbitals may be involved [12]:

i) σ (bonding) molecular

ii) π (bonding) molecular orbital

iii) n (non-bonding) atomic orbital

In addition, two types of anti-bonding orbitals may be involved in the transition:

i) σ* (sigma star) orbital

ii) π* (pi star) orbital

(There is no such thing as an n* antibonding orbital as the n electrons do not form bonds).

A transition in which a bonding s electron is excited to an antibonding σ orbital is referred to as σ to σ* transition. The π to π* transition is the transition of one of the electron of a lone pair (non-bonding electron pair) to an antibonding π orbital. Thus the following electronic transitions can occur by the absorption of ultraviolet and visible light shown in Fig.1.2

σ to σ*,

n to σ*

n to π*

π to π*.

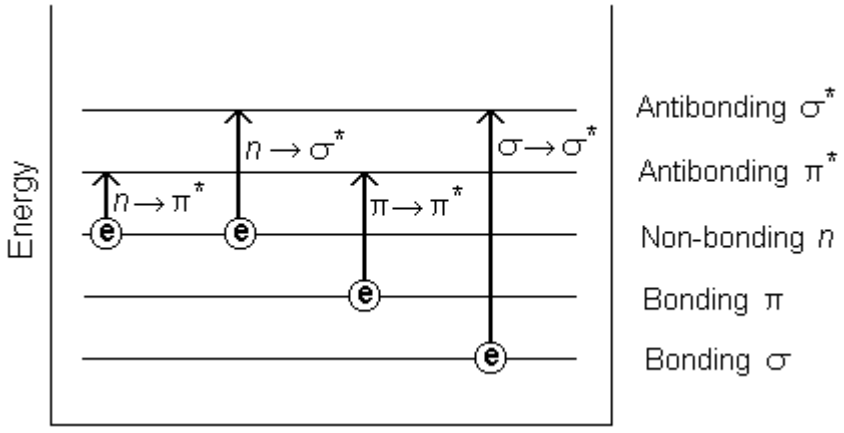

Fig: 1.2 Diagrammatic representation of molecular transitions.

Both s to σ* and n to σ* transitions require a great deal of energy and therefore occur in the far ultraviolet region or weakly in the region 180-240nm. Consequently, saturated groups do not exhibit strong absorption in the ordinary ultraviolet region. Transitions of the n to π* and π to π* type occur in molecules with unsaturated centers; they require less energy and occur at longer wavelengths than transitions to σ* anti-bonding orbitals. Many inorganic species show charge-transfer absorption and are called charge-transfer complexes. For a complex to demonstrate charge-transfer behaviour, one of its components must have electron donating properties and another component must be able to accept electrons. Absorption of radiation then involves the transfer of an electron from the donor to an orbital associated with the acceptor. Molar absorption coefficient from charge-transfer absorption are large (greater that 10,000 L mol^{-1} cm^{-1}).

1.5.3 FTIR

The application of traditional infrared spectroscopy to low concentration measurements, such as ambient air measurements, is limited by several factors. First is the significant presence of water vapour, CO_2 and methane, which strongly absorb in many regions of the infrared (IR) spectrum. Consequently, the spectral regions that can easily be used to search for pollutants are limited to 760-1300cm -1, 2000-2230 cm -1 , and 2390-3000 cm -1 . Another problem is that the sensitivity is not enough to detect very small concentrations in the sub-ppm level. Finally, spectral analysis was difficult since subtraction of background spectra had to be carried out manually.

The development of Fourier Transform Infra-Red spectroscopy (FTIR) in the early 1970s provided a quantum leap in infrared analytical capabilities for monitoring trace pollutants in ambient air. This technique offered a number of advantages over conventional infrared systems, including sensitivity, speed and improved data processing.

Fig. 1.3: Basic components of FTIR

The basic components of an FTIR are shown schematically in Figure 1.3 The infrared source emits a broad band of different wavelength of infrared radiation. The IR source used in the Temet GASMET FTIR CR-series is a SiC ceramic at a temperature of 1550 K. The IR radiation goes through an interferometer that modulates the infrared radiation. The interferometer performs an optical inverse Fourier transform on the entering IR radiation. The modulated IR beam passes through the gas sample where it is absorbed to various extents at different wavelengths by the various molecules present. Finally the intensity of the IR beam is detected by a detector, which is a liquid-nitrogen cooled MCT (Mercury-Cadmium-Telluride) detector in the case of the Temet GASMET FTIR CR-series. The detected signal is digitized and Fourier transformed by the computer to get the IR spectrum of the sample gas.

The unique part of an FTIR spectrometer is the interferometer. A Michelson type plane mirror interferometer is displayed in Figure 1.4 Infrared radiation from the source is collected and collimated (made parallel) before it strikes the beam-splitter. The beam splitter ideally transmits one half of the radiation, and reflects the other half. Both transmitted and reflected beams strike mirrors, which reflect the two beams back to the beam splitter. Thus, one half of the infrared radiation that finally goes to the sample gas has first been reflected from the beam splitter to the moving mirror, and then back to the beam splitter. The other half of the infrared radiation going to the sample has first gone through the beam splitter and then reflected from the fixed mirror back to the beam splitter. When these two optical paths are reunited, interference occurs at the beam splitter because of the optical path difference caused by the scanning of the moving mirror.

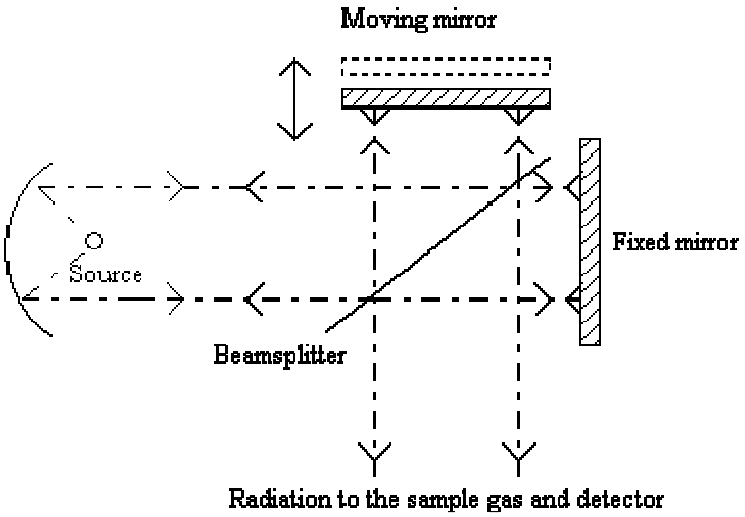

Fig. 1.4: Michelson interferometer

The optical path length difference between the two optical paths of a Michelson interferometer is two times the displacement of the moving mirror. The interference signal measured by the detector as a function of the optical path length difference is called the interferogram. A typical interferogram produced by the interferometer is shown in Figure 1.5. The graph shows the intensity of the infrared radiation as a function of the displacement of the moving mirror. At the peak position, the optical path length is exactly the same for the radiation that comes from the moving mirror as it is for the radiation that comes from the fixed mirror

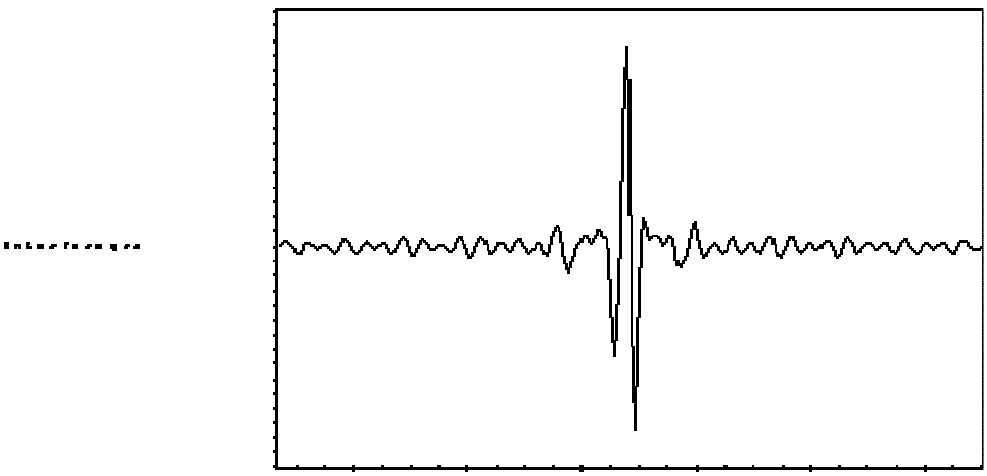

Fig 1.5: A typical interferogram.

The spectrum can be computed from the interferogram by performing a Fourier transform. The Fourier transform is performed by the same computer that ultimately performs the quantitative analysis of the spectrum.

The degree of absorption of infrared radiation at each wavelength is quantitatively related to the number of absorbing molecules in the sample gas. Since there is a linear relationship between the absorbance and the number of absorbing molecules, multi-component quantitative analysis of gas mixtures is feasible.

To perform multi-component analysis we start with the sample spectrum. In addition, we need reference spectra of all the gas components that may exist in the sample, if these components are to be analyzed. A reference spectrum is a spectrum of one single gas component of specific concentration. In multi-component analysis we try to combine these reference spectra with appropriate multipliers in order to get a spectrum that is as close as possible to the sample spectrum. If we succeed in forming a spectrum similar to the sample spectrum, we get the concentration of each gas component in the sample gas using the multipliers of the reference spectra, provided that we know the concentrations of the reference gases.

The mentioned characterization techniques are applied on the biomaterials under purview of this present thesis. The detail outcome of characterization results obtained, for the biomaterial, along with their analysis and conclusion are discussed in the following chapters.

1.5.4 AFM

Principle of Atomic force microscopy

Atomic force microscopy (AFM) is a very high-resolution type of scanning probe microscopy, with demonstrated resolution on the order of fractions of a nanometer, more than 1000 times better than the optical diffraction limit. The AFM is one of the foremost tools for imaging, measuring, and manipulating matter at the nano-scale. The information is gathered by "feeling" the surface with a mechanical probe. Piezoelectric elements that facilitate tiny but accurate and precise movements on (electronic) command enable the very precise scanning. In some variations, electric potentials [13] can also be scanned using conducting cantilevers. In newer

more advanced versions, currents can even be passed through the tip to probe the electrical conductivity or transport of the underlying surface, but this is much more challenging with very few groups reporting reliable data.

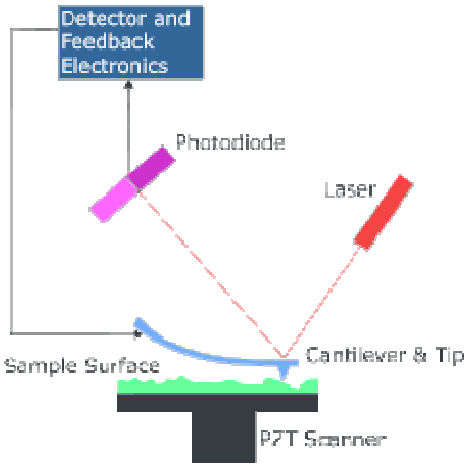

Fig 1.6: Ray-diagram of AFM.

The AFM consists of a cantilever with a sharp tip (probe) at its end that is used to scan the specimen surface. A ray-diagram of AFM is shown in fig 1.6. The cantilever is typically silicon or silicon nitride with a tip radius of curvature on the order of nanometers. When the tip is brought into proximity of a sample surface, forces between the tip and the sample lead to a deflection of the cantilever according to Hooke's law. Depending on the situation, forces that are measured in AFM include

mechanical contact force, van der Waals forces, capillary forces, chemical bonding, electrostatic forces, magnetic forces (see magnetic force microscope, MFM), Casimir forces, solvation forces, etc. Along with force, additional quantities may simultaneously be measured through the use of specialized types of probe (see scanning thermal microscopy, photo-thermal micro-spectroscopy, etc.). Typically, the deflection is measured using a laser spot reflected from the top surface of the cantilever into an array of photodiodes. Other methods that are used include optical interferometry, capacitive sensing or piezo-resistive AFM cantilevers. These cantilevers are fabricated with piezo-resistive elements that act as a strain gauge. Using a Wheatstone bridge, strain in the AFM cantilever due to deflection can be measured, but this method is not as sensitive as laser deflection or interferometry.

If the tip was scanned at a constant height, a risk would exist that the tip collides with the surface, causing damage. Hence, in most cases a feedback mechanism is employed to adjust the tip-to-sample distance to maintain a constant force between the tip and the sample. Traditionally, the sample is mounted on a piezoelectric tube, that can move the sample in the *z* direction for maintaining a constant force, and the *x* and *y* directions for scanning the sample. Alternatively a 'tripod' configuration of three piezo crystals may be employed, with each responsible for scanning in the x, y and z directions. This eliminates some of the distortion effects seen with a tube scanner. In newer designs, the tip is mounted on a vertical piezo scanner while the sample is being scanned in X and Y using another piezo block. The resulting map of the area $s = f(x,y)$ represents the topography of the sample.

The AFM can be operated in a number of modes, depending on the application. In general, possible imaging modes are divided into static (also called *contact*) modes and a variety of dynamic (or non-contact) modes where the cantilever is vibrated.

1.6 Dielectric and magnetic aspects.

Frequency dependent a.c. electrical conductivity conductivity

A typical variation of A.C. electrical conductivity [14] of a specimen with applied A.C. is analogous to as shown in Figure 2.10. The experimental A.C. conductivities are calculated from the measured data (Z: value of impedance and θ: phase angle), following relation,

$$\sigma_{ac}(\omega) = (d/RA) \quad (1.6)$$

Where, R is the real part of the impedance, d is the sample thickness and A is the cross-sectional area (CSA) of the electrodes. The variation of A.C. conductivity with frequency ω may be described following Jonscher's power law [14] viz.

$$\sigma_{\omega} = \sigma_{dc} + K\,\omega^{n} \quad (1.7)$$

$$\text{Or, } \log(\sigma_{\omega} - \sigma_{dc}) = n \log \omega + \log K \quad (1.8)$$

Where 'K' and 'n' are the temperature dependent, frequency independent material parameters required to be estimated. Value of n may be directly estimated from the slope of the above equation.

Magnetic Measurements

Several methods may be used for magnetic susceptibility measurement such as Faraday's scale, Guoy's scale or inductive method with Superconducting Quantum Interference Device (SQUID) magnetometer and popular VSM [15] method. A comprehensive survey of the method is discussed by Marcon and Ostanina [16]. The magnetic data was obtained using a SQUID. SQUID principle [17] is based on flux quantization and Josephson tunneling through a weak coupling.

The prime advantage of a SQUID is to make extremely sensitive measurements of magnetic fields. The SQUID method can measure a magnetic moment within a wide range and with high precision. There exists variety of SQUID set up which are used in laboratories. In VSM technique specimen is placed inside a uniform magnetic field to

magnetize the sample. The sample is then physically vibrated sinusoidally, typically through the use of a piezoelectric material. Commercial systems use linear actuators of some form, and historically the development of these systems was done using modified audio speakers, though this approach was dropped due to the interference through the in-phase magnetic noise produced, as the magnetic flux through a nearby pickup coil varies sinusoidal way. The induced voltage in the pickup coil is proportional to the sample's magnetic moment, but does not depend on the strength of the applied magnetic field. In a typical setup, the induced voltage is measured through the use of a lock-in amplifier using the piezoelectric signal as its reference signal. By measuring in the field of an external electromagnet, it is possible to obtain the hysteresis curve of a material. Magneto-optical Kerr effect magnetometer (MOKE) [18] designed for hysteresis loop measurements of mono-atomic layers and spintronics nanostructures. For obtaining full information about magnetization reversal process in magnetic multilayer both magnetometers should be used, because both methods are complementary. R-VSM measurements deliver information about averaged magnetization process from the whole volume of the sample, whereas magneto-optical information from MOKE magnetometer is local, limited by light-beam spot and depth with an exponential decay be found in literature. This technique measures surface magnetism of a specimen in contrast to other technique which measures bulk magnetism. Induction method of magnetic measurement is also popular. Coillot and Leroy [19] provide a good survey on magnetic sensor based on it.

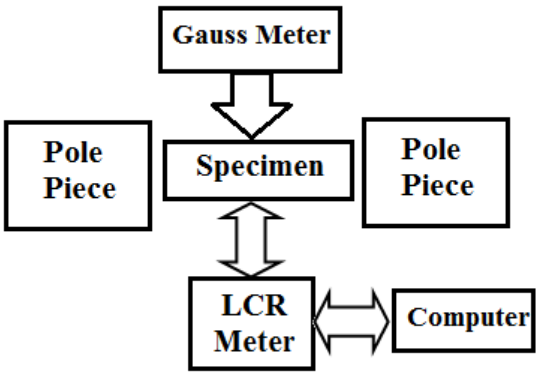

Fig.1.7. Simple layout of experimental setup of magnetic susceptibility at RT.

The principle of induction sensor directly based on Faraday's law of electro-magnetic induction. The voltage output is proportional to the time derivative of the

total magnetic flux, and it is essentially an a.c. method. The present technique of magnetic measurement makes use the principle if variation self inductance of a coil. The experimental specimen is placed inside the core of the coil. The arrangement when subjected to external longitudinal d.c. magnetic field the self inductance of the coil changes in accordance to the magnetization of the specimen. The details of the principle, experimental technique, analysis and results are discussed in the following sections.

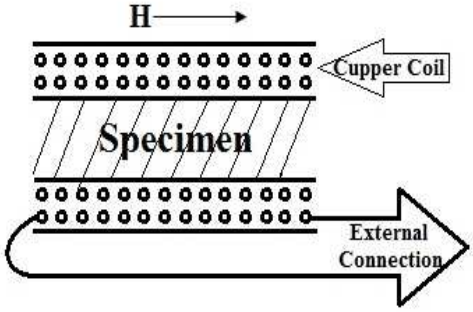

Fig.1.8. Sample core design

Self inductance of a small hollow copper coil is measured in this technique. The self inductance per unit length of the coil is given by,

$$L_0 = k\,\mu_0\pi\, r_1^2\, n^2 \qquad (1.9)$$

r_1 is the mean radius of the coil with n numbers of turn and k is a geometrical. Specimen of magnetic material when inserted in its core the self inductance of the arrangement as shown in Fig.1.8 is given by,

$$L = k[\mu_0\pi(r_1^2 - r_2^2) + \mu_0\,\mu_r\,\pi\, r_2^2]\, n^2 \qquad (1.10)$$

Where r_2 is the radius of the core material and μ_r is its relative permeability. Then the magnetic susceptibility of the specimen is given by,

$$\chi_m = \mu_r - 1 = k\,(L - L_0)/\,L_0 \qquad (1.11)$$

where k is geometrical constant given by,

$$k= (r_1/ r_2)^2 (l_1/l_2)^2 \lambda \qquad (1.12)$$

where, l_1 and l_2 ($l_2 < l_1$) are the lengths of the coil and specimen respectively. The quantity λ is the calibration factor.

The self inductances L_0 and L can be measured by LCR meter with high precision. Following principle of Impedance Spectroscopy[7], by the application of small sinusoidal emf which does not disturb the equilibrium of the specimen, L can be measured directly. Application of d.c. longitudinal magnetic field (H) on the specimen will cause a change in magnetization in it. The change in magnetization (M) is equivalent to change in its susceptibility (χ_m) and hence the self inductance L. In general the magnetization M of a non-linear material is given by,

$$M= M_0 + M_1H + M_2 H^2 + \ldots \qquad (1.13)$$

References.

1. V. Dimitrov1, T. Komatsu, J. Univ. Chem. Tech. & Metall. 45, 3, 2010, pp219-250.
2. V. Dimitrov1, T. Komatsu J. Solid State Chem. 163.2002,100 ; V. Dimitrov and S.Sakka, J. Appl. Phys, 79, 1996, pp1736
3. Tian Yu-Feng et al, Chin. Phys. B Vol. 22, No. 8 (2013) 088505, Bednorz J G and Mller K A 1986 Z. Phys. B 64 pp189.
4. Jin S, Tiefel T H, McCormack M, Fastnacht R A, Ramesh R and Chen L H 1994 Science 264 pp413.
5. King P D C and Veal T D 2011 J. Phys.: Condens. Matter 23 334 pp214
6. Izyumskaya N, Alivov Ya and Morkoc¸ H 2009 Crit. Rev. Solid State Mater. Sci. 34 89
7. www.molecularinfo.com/MTM/UV.pdf cited at 02/12/10.
8. E. L. Nagaev, Uspekhi Fizicheskih Nauk (in Russian (/English) 1996 166 (8) pp833 858. doi:10.3367/UFNr.0166.199608b.0833.
9. C. N. R. Rao, and B. Raveau, eds. *Colossal Magnetoresistance, Charge Ordering and Related Properties of Manganese Oxides.* World Scientfic Publishing Co. p. 2. ISBN 978-981-02-3276-4, (1998).

10. G. H. Jonker and J. H. Van Santen, Physica 16 1950, p 337
11. M. Julliere, Phys. Lett. 54A (1975) pp225–226.
12. Peter Eaton and Paul West, Atomic force microscopy, Oxford University Press, 2010.
13. H.Mallick and A.Sarkar, Bull Mater Sci, 23 2000 pp319-324.
14. A.K. Jonscher, Nature, 267 1997 pp23.
15. S.Foner, Rev. Sci. Instrum 30 (7) pp548–557.
16. PIERS Proceedings, Kuala Lumpur, MALAYSIA, March,27{30, 2012, pp420-424.
17. R. L. Fagaly, Superconducting quantum interference device instruments and application Rev. Sci. Instrum, 2006, 77, 101101.
18. J. Wrona, T. Stobiecki, R. Rak, M. Czapkiewicz, F. Stobiecki, L. Uba, J. Korecki, T. ! Sl)ezak, J. Wilgocka- Sl)ezak, M. Roots, Kerr magnetometer based on a differential amplifier Phys. Stat. Sol. (A) 196 (1) 2003 pp161-164.
19. C. Coillot and P. Leroy, Induction Magnetometers Principle, Modeling and Ways of Improvement, Magnetic Sensors Principles and Applications, Ch-3, Dr Kevin Kuang (Ed.), ISBN: 978-953-51-0232-8, InTech. 2012.

Chapter-2

Characterization of confined Sol-Gel synthesized NiS nano-clusters.

2.1 Introduction

In the past organic-inorganic nano-composite becomes most interesting field of research [1, 2] in 'Solid State Physics' for their superior physical properties. The drastic change in the electrical, electronic and magnetic properties of the quantum sized nano system over its bulk counterpart due to interfacial interaction between nanostructure and external environment has considerable interest in modern science and technology [3-5]. The role of ion-conducting capping medium in synthesis of nano-materials and the properties of the material are studied. But it is rare to emphasize so far on period of retaining of the properties of the nano-materials, which is very important in the nano-electronics, nano-photonic device and biomedical technology. High attention has been paid on the 'oxide' nano-particles due to their applicability in many practical applications leaving a little attention on sulphide nano clusters. The objective of this work is to develop Nickel Sulphide nano-clusters, its nano-composite with Gum Arabica and to investigate their material characteristics.

The Nickel Sulphide is known as magnetic semiconductor although its nature of magnetism in the form of nano-composite is complicated. Nickel Sulphide is a photo-sensitive [6] material and may be used in photo-energy generation. A series of recent activity [6] demonstrating controllable fabrication of magnetic semiconductors and their incorporation into hetero-structures has led to several additional device suggestions. They include a spin filter, spin-resonant-tunneling diode, unipolar spin transistor, magnetic Zener tunnel diode and magnetic p-n diode. At the same time, progress on the problem of spin injection into nonmagnetic semiconductors has been reported, both from magnetic semiconductors and from magnetic metals. Electrical resistivity measurements [7] on the NiS system show that it has a high metallic conductivity (2×10^4 Ohms−1-cm−1) at room temperature. In this work Gum Arabica, a biopolymer has been used to develop nano-composite of Nickel Sulphide

for AFM study. Gum Arabica [8, 9] has been found from different species of Acacia namely Acacia Arabica, Acacia babul etc. The details of the experiments, results and analysis are given in the following sections.

2.2 Experimental

Sample preparation

In this work a natural self assembly of NiS nano-cluster was undertaken. The chemical sol gel route was chosen with Ni salt, Nickel carbonate compound, $NiCO_3$, $2Ni(OH)_2,4H_2O$, from E-mark India, boiled in ammonia solution at temperature about 100^0C. Filtering the sample, mixed with liquid ammonia (NH_3) solution and gum acacia powder heated in magnetic stirrer and slowly passing H_2S gas through it .The formation of NiS nano-cluster is achieved by natural self assembly in polymeric background of Gum Arabica biopolymers. The Ni_2S_3 specimen was developed using Ni (III) acetate in acetic acid medium following the mentioned chemical process. The composite of nano cluster was caste to develop the experimental sample. They were caste in smooth extended surface so as to ensure a minimum thickness. Finally the specimens were adequately to dry properly. The thickness of the specimen produced was approximately 0.7mm. Specimens were also developed, without polymeric background, for XRD, FTIR and Optical experiments.

Test and Measurements

The different experimental tools those used for test and measurements were, XRD and AFM analysis - which are important experiment for study morphological nature of the specimen. The experiments were carried out to characterize the material are d.c I-V characteristics and conductivity measurement, Optical Absorption Spectroscopy using UV-VIS spectrophotometer and FTIR spectrophotometer to investigate energy band gap in developed nano-clusters, and magnetic moment measurement for investigation of the magnetic nature of the developed nano composite of NiS nano-clusters.

2.3 Results and discussions.

2.3.1 XRD Analysis

XRD analysis of the developed specimen is carried out to examine its microstructure, morphology and is completed with Phillips PW1710 automatic diffractometer. XRD intensity distribution curve of the examined sample are shown in the Fig. 2.1 The overall radial distribution function peak of the diffraction pattern corresponds to $2\theta = 38.83^{o}$.

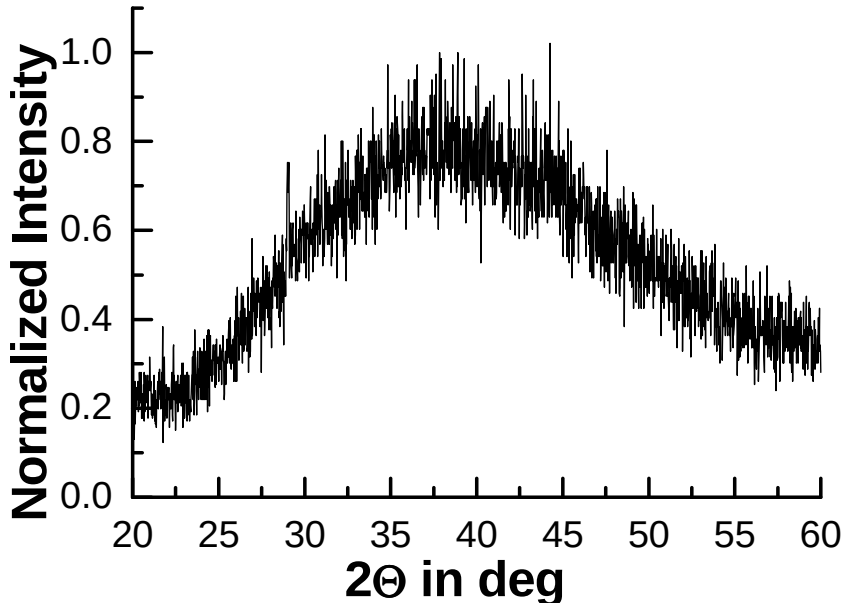

Figure 2.1 XRD pattern of the NiS nano-composite between 2θ ranges 20-60 deg.

From this intensity distribution by using Scherrer equation we obtain the particle size as $L = (0.9\ \lambda)/\{Cos\theta_b\ (\Delta 2\theta_b)\}$ Å, where λ is the wavelength of the X-ray radiation and for Cu K_α is equal to 1.5418 Å, θ_b is the glancing angle and $\Delta 2\theta_b$ is the difference in the angle at the two end of full width half maxima. The results do not show any Sharpe peak of the intensity distribution but an overall peak corresponding to $2\theta = 38.83^{o}$. In the neighborhood of $2\theta = 38.83^{o}$, there are discrete peaks which are relatively low intensities. These peaks are exploited to calculate the particle size using Scherrer Equation [10], and it has been found that the size vary between 40 – 90 nm. The overall impression of the XRD analysis of the developed specimen is a nano-composite of NiS cluster. The overall nature is amorphous due to background bio-polymeric material and NiS clusters. It can be asses that small grain size caused the

surface roughening to increase. It is also responsible for destroying the crystalline nature. Due to the smaller grain size and their large number density, the grain boundary effect becomes predominant in the composite. This forms surface defect that affects the structural and morphological property.

2.3.2 AFM Analysis

AFM study of NiS nano-clusters in bio-polymeric background was carried out using AFM model NANOSCOPE F (USA). The AFM photograph is shown in Fig.2.2

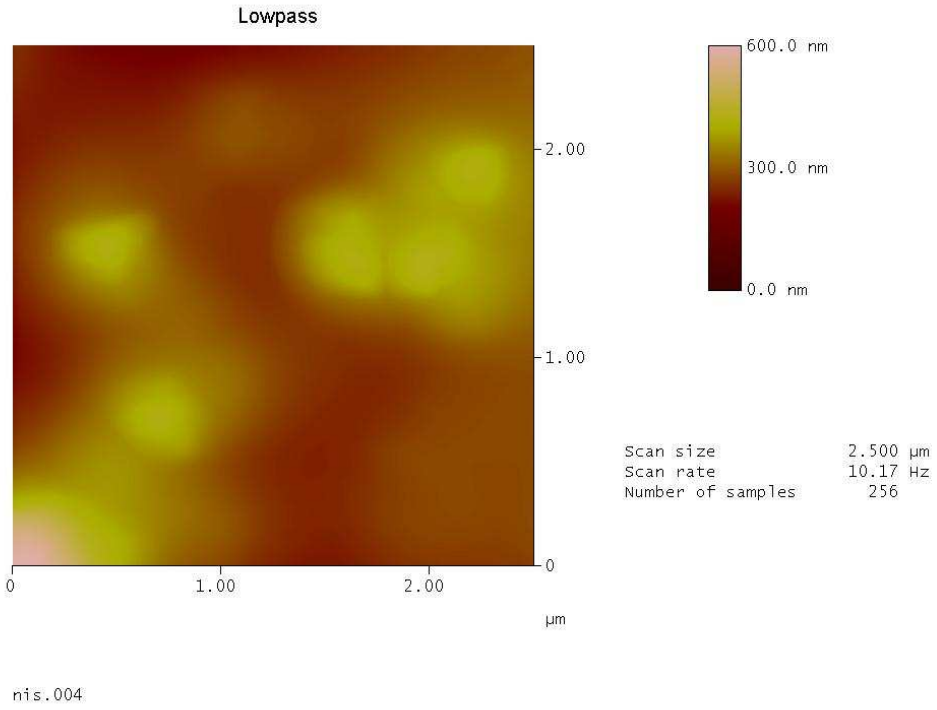

Figure 2.2 AFM microgram of NiS nano-clusters in bio-polymeric background.

Fig. 2.2 shows the AFM results of NiS nano-clusters of size ranging between 30-50 nm. The estimated of NC's in bio-polymeric background are larger compared to those developed without bio-polymeric background.

2.3.3 Optical Absorption Spectroscopy

UV-VIS absorption spectra of the specimens NiS and Ni_2S_3 pellet specimens were studied with UV-2450 UV-VIS spectrophotometer, Shimadzu, Japan in the range between 190nm to 900nm at adequate accuracy using integrating sphere attachment and compensating $BaSO_4$ background. The results of the study between 190-300 nm are shown in Fig.2.3

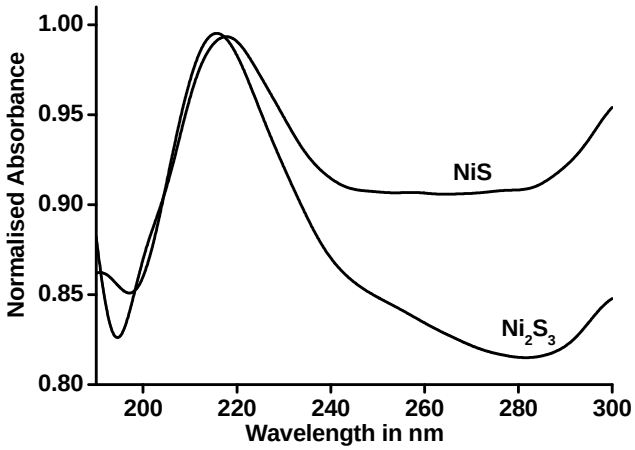

Figure 2.3 UV-VIS absorption spectra of NiS and Ni_2S_3.

2.3.4 FTIR Analysis

The infra red (IR) absorption of NiS and Ni_2S_3 powder specimen provides information [11] about energy difference due to electronic transition or vibration states originating from bond bending, bond stretching of molecular constituents of the specimens. The analysis was carried out using FTIR model, IR affinity 1, Shimadzu, Japan, at high resolution (resolution was 1 cm^{-1}) using KBr window. IR absorption for a molecule provides information about energy difference between vibrational states, originating from bond bending and bond stretching. Fig. 2.4 shows the FTIR vibrational spectrum of the developed complex and also compared to that of the pure Gum Arabica. The functional group region appears from 4000 cm^{-1} to about 1550 cm^{-1}. The results obtained from Fig. 2.4 shows evidence of direct band gap of the

specimens in IR region .The estimated direct Band Gap of NiS is 0.28eV and that of Ni_2S_3 is 0.12eV respectively. Anuar et al [12] studied the optical absorption of their developed NiS by sol-gel process and the estimated band gap measured to be 1.3 eV. Sartale and Lokhande [13] reported that Nickel sulphide has a band gap of approximately 0.5 eV

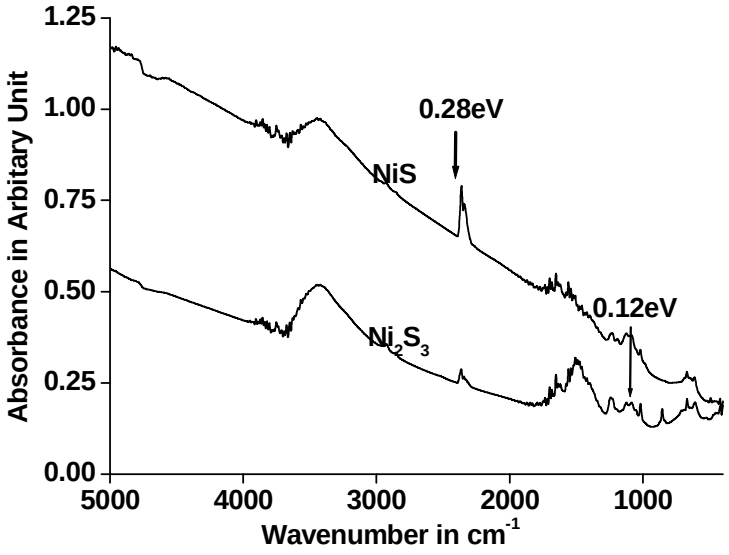

Figure 2.4 FTIR absorption spectra of NiS and Ni_2S_3.

2.3.5 d.c I-V Characteristics

For the experiment of d.c I-V characteristics the sample was sandwiched between two high polished flat copper plates act as electrodes for electrical measurement. The applied field direction was perpendicular to the 2-D plane of the specimen. The d.c I-V characterization of the specimens at room temperature was carried out using by Keithley 2400 Source meter (USA) and plotted using characterization software. The overall nature of I-V characteristic is an apparent indicator of formation of localized energy level of the NC's in host background matrix. The conductance (G) of the specimen was estimated and plotted as a function of applied voltage (V) as shown in Fig. 2.5 The formation of localized energy level in

the recorded I-V characteristic may be attributed due to 3-D confinement [14,15] of quantum dot like ionic nano-cluster within the dielectric host.

The following noise in the mesoscopic systems [16] the observed nature of the conductance plot shown in Fig.2.5 appeared to be like that of a telegraph noise. In fact it arises due to transition between two locally stable states at room temperature (RT). The nature of the conductance variation is due to presence of quantum dots in the system later gives rise to Coulomb Blockade effect [17]. The observed conductance fluctuation is thus a direct evidence of presence of nano-clusters in the system. In this experimental result, the observed noise appeared as an admixture of Nyquist – Johnson, shot noise and 1/f types of noise originating mostly from the quantum confinement of 3D nano-clusters in the specimen. Apparent nature of conductance fluctuation is the indicator of formation of localized energy levels in host background.

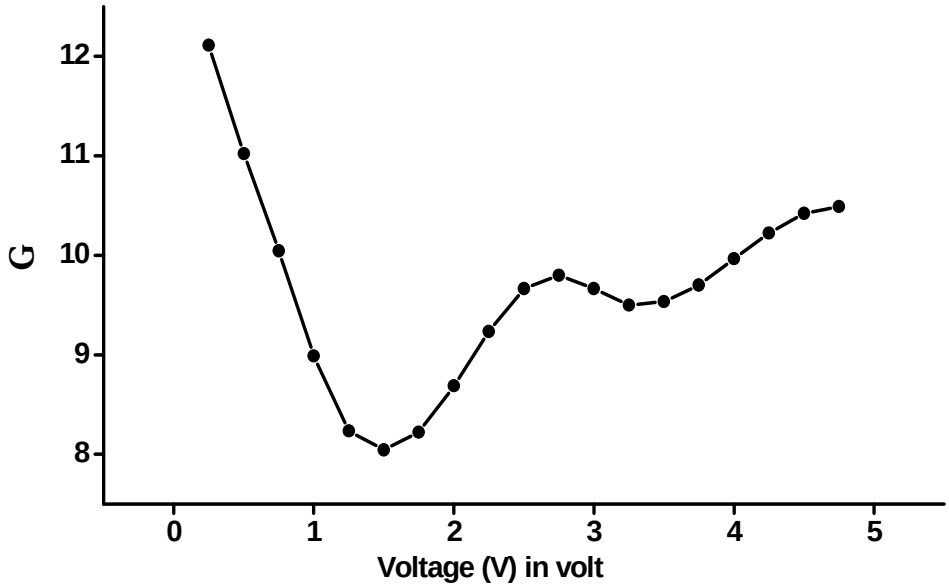

Figure 2.5 Conductance (G) variation of NiS with applied p.d at RT.

There are plateau regions in conductance curve shown by Fig. 2.5 the plateaus occur when the conduction process is terminated i.e. here we try to explain the disorder in the sample. This disorder affect the Landau levels broaden into landau bands. As well as the disorder potential is weak i.e. we mean to say the quantum confinement and the Landau bands are merge to continuum . In strong disorder the localized states are predominates and passing of information through electron is

prohibited. Since the localization length of a cluster is small, the overlapping of adjacent wave functions are not strong, so one may get plateaus that is conduction enhancement does not takes place. Due to the introduction of nano-cluster in the specimen the ionic conductivity is found to increase over the pure polymer. Similar effect [18] has been observed in ionic conduction of solids with nano-filler. At room temperature it behaves as a small band gap semiconductor and at room temperature exhibits electrical noise like appearance as marked characteristics of nano-composite. The NiS nanoclusters are distributed in the polymeric matrix of Gum Arabica, and there exists size distribution also. Since the density of states in nano regime are much smaller than that of bulk one, by altering the size of the particles means the extension of effective potential, which may easily change the band gap. It is interesting to note that within a nano-composite there are three types of energy band gap probably due to presence of other form of Nickel sulphide.

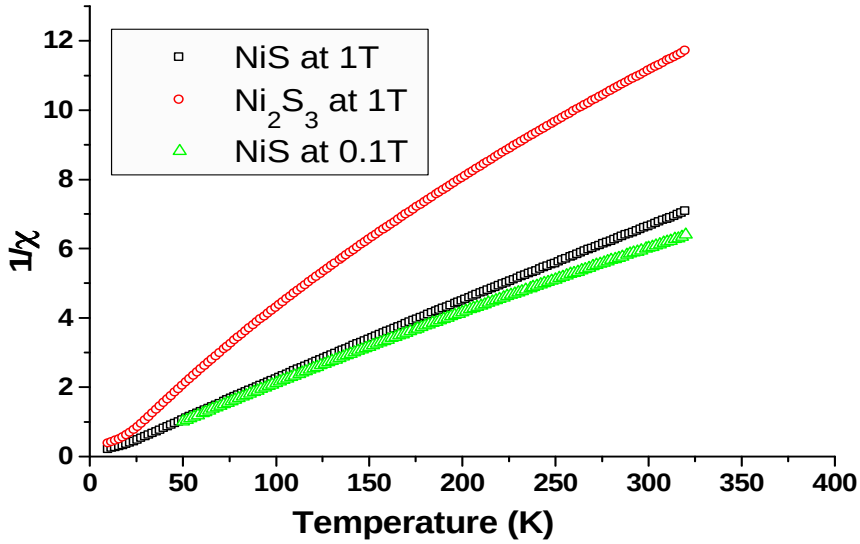

Figure 2.6 Variation (1/χ) with temperature for Nickel Sulphides at mentioned magnetic field.

2.3.6 Magnetic Measurement

NiS and Ni_2S_3 were prepared by chemical synthesis to develop black experimental specimens. The dried sample of Nickel Sulphides was crushed into fine

powder. The magnetic moment of the specimens were measured between temperatures 10-300 K with external magnetic field as parameter. The said measurement was carried out in VSM model Quantum Design (USA). The magnetization/gm of the specimens (M) is recorded as a function of temperature between the temperature range10-300 K at two different fields 0.1 T and 1.0 T. The results thus obtained are shown in Fig. 2.6. The measured M shows variation with fields and temperature as well. It has been found that temperature between RT to 40 K magnetic behaviour is paramagnetic and that between 40K to 10K the specimen appeared as ferromagnetic however there exists no sharp phase transition. Thus overall magnetic nature of disordered nano sized NiS clusters appeared to be complicated in nature. The value of observed magnetic susceptibility (χ) of the Ni_2S_3 specimen shows a weak ferromagnetic in nature however ordered NiS bulk solid is known to be an anti-ferromagnetic material. The values of χ from this present study may be due to presence of other sulphide of Nickel in the form Ni_xS_y. The nature of magnetism in the later is not properly known. Thus overall magnetic nature of disordered nano sized NiS clusters appeared to be very complicated in nature. The value of observed susceptibility χ shows a paramagnetic in nature however ordered NiS bulk solid is known to be an anti-ferromagnetic material. Fig. 2.7 shows(the significant portion of the measured data are shown) an exclusive characteristic variation of magnetic susceptibility of Ni_2S_3 with temperature measured at 1.0T field. The region between arrow mark the behavior of the specimen appears to be ferromagnetic and temperature above 30 K the specimen is paramagnetic. The Ni_2S_3 specimen is however showed a super-paramagnetic in nature.

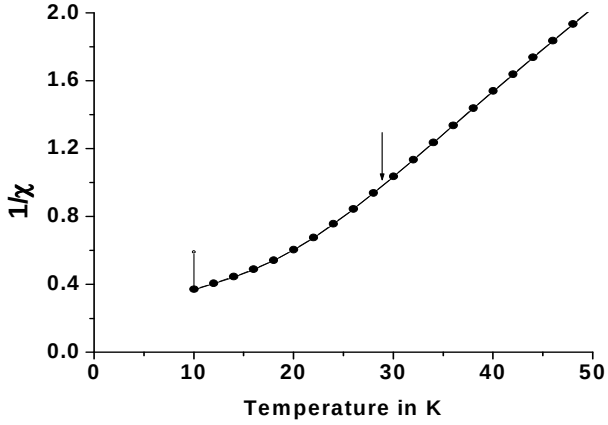

Figure 2.7 Variation of (1/χ) with temperature at 1.0 T magnetic field for Ni_2S_3 specimen.

The nature of magnetism in Nickel Sulphide is complicated and interesting. Following analysis of experimental data Coley et al [19] showed that nickel sulphide has temperature dependent magnetic susceptibility and has an itinerant-electron anti-ferromagnet with no local moment. Wei Wang et al [20] showed from a hysteresis scan of NiS Nano Tube that there exists a weak ferromagnetism at room temperature. In the work [20] the observed value of magnetic permeability-μ shows a weak ferromagnetic nature however ordered NiS bulk solid is known to be an anti-ferromagnetic material.

Nanomagnetism is a highly interesting subject of solid state magnetism and nanotechnology [21-23]. The novel phenomena super-paramagnetism and its effects appear only on the nanoscale. The present nano Ni_2S_3 specimen is however showed a super-paramagnetic in nature without any sharp transition.

2.4 Application potential of NiS:

Infra-Red(IR) absorption of Nickel Sulphide complex.

2.4.1 Introduction

About 45%of the solar energy reaching earths surface lies in the near infrared region of the spectrum. Most existing solar panel have only effectively harnessed light energy while allowing nearly half of the energy in spectrum (in the form of infrared waves) to passed by mostly unused because conventional silicon based solar cell are

unable to harness the infrared radiation. The need to develop inexpensive renewable energy sources stimulates scientific research for efficient, low-cost photovoltaic devices. The biopolymer-based photovoltaic elements have introduced at least the potential of obtaining cheap and easy methods to produce energy from light. The possibility of chemically manipulating the material properties of biopolymers combined with a variety of easy and cheap processing techniques has made biopolymer-based materials present in almost every aspect of modern society. In earlier studies [24, 25] it has been found that NiS is a magnetic semiconductor although its nature of magnetism in the form of present nano composite is complicated. Nickel Sulphide is a photo-sensitive [26] material and may be used in photo-energy generation. A series of recent activity [26] demonstrating controllable fabrication of magnetic semiconductors and their incorporation into hetero-structures has led to several additional device suggestions. In this study NiS has been used to harness the infrared region of the light wave. The experimental details and results are discussed in the following sections.

2.4.2 Sample Preparation

In the present work we deal with a natural self assembly of NiS nano-cluster in conducting background of biopolymer. The biopolymer Gum Arabica [8] powder is used as a capping medium for the preparation of experimental specimen. At first we take Ni salt i.e Nickel Carbonate of $NiCO_3$,$2Ni(OH)_2$,$4H_2O$ from E-mark India and boiled in amoniacal water at temparature about 100C Filtering the sample, mixed with liquid Ammonia (NH_3) solution and gum acacia powder heated in magnetic sterier and slowly passing H_2S gas through it . Hence the formation of NiS nano specimen by natural self-assembly is in the background of Gum arabica biopolymers.

2.4.3 Experimental

In this work both d.c I-V characteristics and a.c measurements are carried out. In earlier study [26] it has been found that the developed particle size by using is almost between 4 – 9 nm. The overall nature is amorphous due to background bio-polymeric material. The d.c I-V characteristics are recorded at room temperature with voltage step 10mV between -0.2 to +0.2V. The measurement is carried with the specimen

exposed to IR radiation from IR diode MLED 930. I-V data for the specimen was also recorded under exposure to IR from enclosed radiator at 60 C. The d.c measurements are carried out using PC interfaced Keithley 2400 series source meter. The investigation of total electrical conduction of the developed NiS complex of Gum Arabica specimen was carried out, between frequency range 1 Hz to 100 KHz HIOKI 3522 LCR/Z Analyzer (Japan).

2.4.4 Results and Discussions

Fig. 2.8 shows d.c bulk I-V character of NiS composite specimens under IR radiation about 930 nm from IR diode. The fig.2.8 also compared the irradiated result to that at near dark condition. The recorded current is small in magnitude due to small specimen area that exposed to irradiation.

Fig. 2.9 compares the result of d.c I-V on the NiS complex specimen under exposure to IR from enclosed radiator at 60 C to that of with no additional IR radiation The fig.2.9 shows that conductivity in presence of radiation increases by about 10 times over without radiation.

The results of ac investigation are in fig. 2.10 in the form of Cole –Cole plot. The overall nature of the curve shows an effective mix conducting (ionic and electronic contribution) nature of NiS complex specimen.

The increase in current seen from fig. 2.8 and fig. 2.9 is due to the presence of nano particle in the material. The NiS nano particle is capable to absorb energy in the infrared part of the spectrum. In the earlier work [26] it has been reported that the estimated direct Band Gap NiS at 0.28eV. The current enhancement due to selective IR radiation of 930 nm is too small (fig.2.8) however the same is substantial (fig.2.9) when a broad spectrum continuous IR radiation is used.

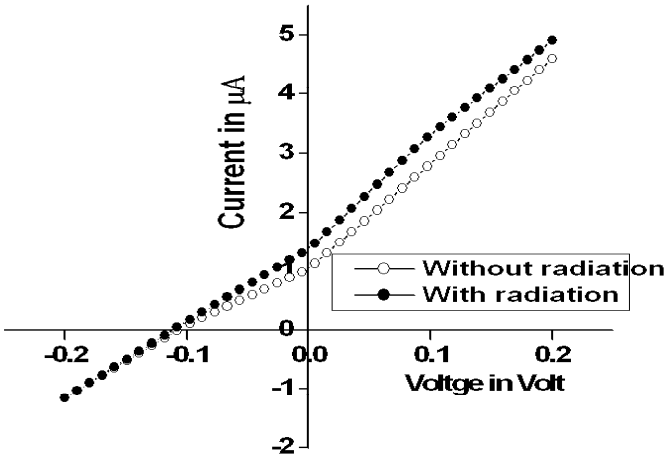

Fig.2.8 d.c I-V characteristics of NiS complex showing its photosensitivity (SampleThickness-1.04mm, Area exposed to radiation =0.13sqcm) at 930 nm IR radiation and without infrared radiation.

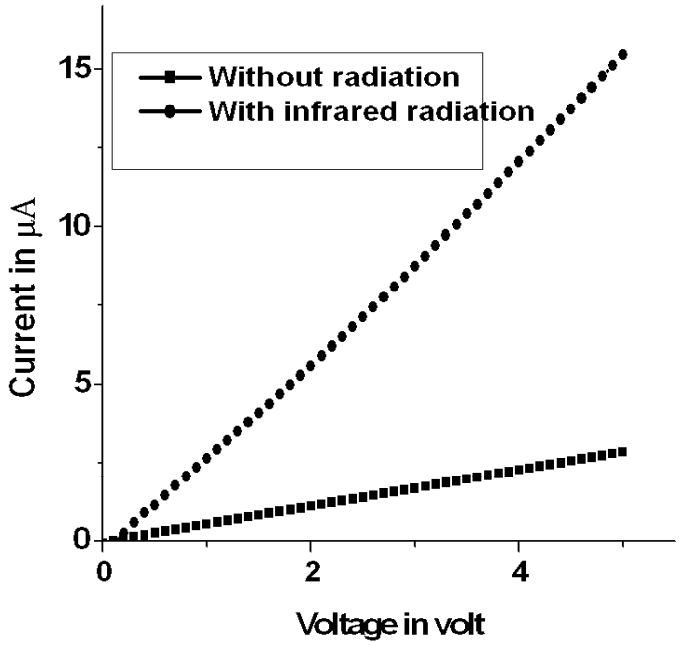

Fig 2.9: d.c I-V characteristics of the developed material with infrared radiation corresponding to 60 C and without infrared radiation. (Thickness-1.74mm. Area-1.32sqcm)

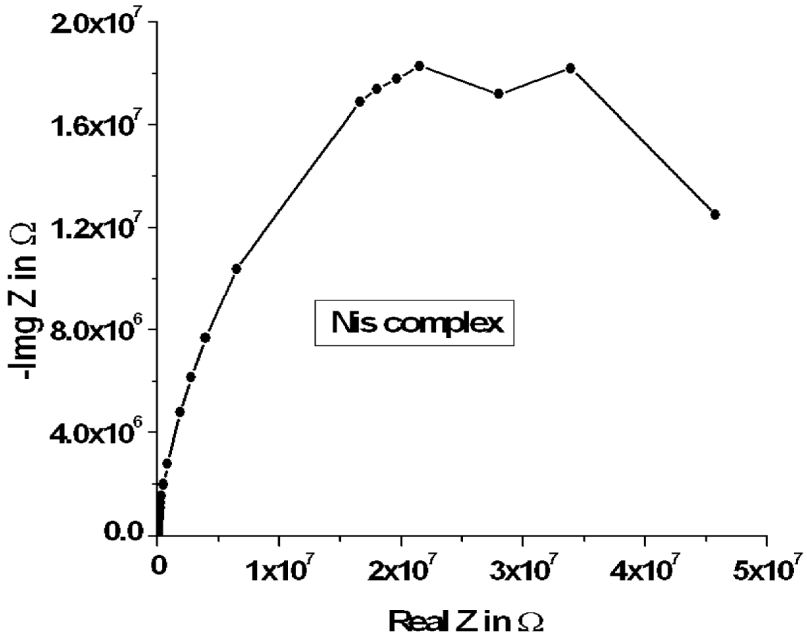

Fig. 2.10 Impedance plot of NiS complex (applied p.d=1v r.m.s).

2.4.5 Conclusion

Formation of ionic nano-clusters (scince a.c impedance analysis shows the substantial contribution of ac conductivity in total electrical conductivity) within polymeric substrate is distinct and clear from I-V characteristic curve. From the study of optical absorption spectroscopy we can assume that as if three type of sized dependent nano-composite formed and it is confirmed that NiS nano-cluster is a the small band gap semiconductor. The overall magnetic nature of the NiS nano composite is amazing. Apart conflicting claim the present study finds a weak ferromagnetism below 40 K and paramagnetic above it in the developed NiS specimen. The scope of further studies on the system may provide many interesting aspect of material science. NiS nano particles can take in energy from both sunlight and the earth's heat radiation with higher efficiency than conventional solar cell. The developed NiS composite successfully exhibits the mentioned property. The overall IR absorbance of the developed NiS complex is observed to be good and encouraging.

References:

1. L. Brus, P. Szajowski, W. Wilson et.al, J.Am. Chem.Soc. 1995,117, pp2915.

2. R. Zallan -Models of Amorphous Solid, J.Non-Cryst. Solids, 1985,75 (No1-3), pp3–14.

3. Y.Alhassid, Rev. Mod. Phys., 2000,72, pp895–968.

4. M.C. Brelle et.al., Pure Appl.Chem., 2000, 72, pp101–117.

5. A.William Johnson, Invitation to Organic Chemistry, John and Bartlet Pub. Toronto,Canada 1999, pp652.

6. T.J.Coutts, M.W. Wanless, J.S. Ward, S. Johnson, 25th IEEE Photovoltaic Specialists Conference, 1996, pp 25.

7. S. R. Krishnakumar, N. Shanthi and D. D. Sarma, arXiv: Cond-mater/0207262v 10 July 2002

8. H. Mallick and A. Sarkar, Bull. Mater. Sci., 2000,23, pp319 – 324.

9. Arup Dutta and A. Sarkar, Adv. Appl. Sci. Res. 2011,2 (1) pp 125-128.

10. B.D. Cullity, Elements of X-Ray Diffraction, Addison-Wesley Publishing Company Inc., Reading, USA, 1956 pp96–100.

11. Mousumi Mukherjee and A. Sarkar, Adv.Appl. Sci. Res. , 2011, 2 (4) pp 407-409.

12. K. Anuar et al, Mat. Sci, 2004,10, no2, ISSN pp 1392-1320.

13. S.D. Sartale, C.D. Lokhande, Mater. Chem. Phys. ,2001,72 pp 101.

14. N. Gupta, H. Mallik and A. Sarkar, J. Metastable and Nano Crystalline Mat., 2005, 23 , pp 335–338.

15. Arnab Gangopadhyay and A. Sarkar, Adv. Appl. Sci. Res , 2011,2 (1) pp 149-152.

16. Yoseph Imry in Mesoscopic physics and Nanotechnology, Introduction to Mesoscopic Physics , 2/e Oxford University Press New York, 1997.

17. M.C. Brelle et.al., Pure Appl.Chem., 72 2000 pp101-117.

18. Ionic Conductivity Enhancement of Polymer Electrolytes with Ceramic Nanowire Fillers,Wei Liu,Nian Liu,Jie Sun Po-Chun Hsu,Yuzhang Li,Hyun-Wook Lee,and Yi CuiNano Lett. 2015,15pp 2740-2745 ; *ibid* Ionic Conductivity enhancement in the Solid Polymer electrolyte PEO9LiTf by nanosilica filler from rice husk ash, M.A.K.L Dissanayake, W.N.S. Rupasingh, J.M.N.I. Jayasundara,P.Ekanayake, T.M.W.J. Bandara,S.N. Thalawala,V.A.Seneviratne. J.S.S Elec.Chem.,June2013,17(6),pp 1775-1783.

19. J.M.D. Coey et al, Phy. Rev. Lett. , 1974, 32 , pp1257–1260.

20. Wei Wang et al , Mat. Sci. Engg., 2006, B 133 , pp167-–171.

21. D. J. Sellmyer and R. Skomski (Eds.), Advanced Magnetic Nanostructures, Springer 2005.

22. B. D. Terris and T. Thomson, Nanofabricated and self-assembled magnetic structures as data storage media, J. Phys. D: Appl. Phys., 2005, 38, pp 199.

23. H.Kronmüller and S. Parkin (eds.), Handbook of Magnetism and Advanced Magnetic Materials (Wiley, Vol. 3, 2007).

24. M Barman, S. S. Pradhan and A. Sarkar Proceedings of 53rd ,DAE Solid State Physics Symposium 2008. pp. 193-194.

25. Moumita Barman, Somnath Paul and A. Sarkar, Adv. Appl.Sci.Res. 2013 4(5) pp. 343-349.

26. T.J. Coutts, M.W. Wanless, J.S. Ward, S. Johnson, 25th IEEE Photovoltaic Specialists Conference, 1996. pp.25.

Chapter-3

Characterization of ZnS Nano-clusters in polymeric background.

3.1 Introduction

ZnS is a very popular efficient phosphor. The ZnS nano-clusters exhibit interesting optical properties [1]. The study of ZnS nano cluster gained importance as a wide band semiconductor. The nano-clusters are generated require capping due to avoid quick degradation or agglomeration. Confinement of the nano-clusters within the polymeric background hinders their degradation or agglomeration. Thin solid films with polymeric background also have the advantage in the field of optical devices. A quantum dot (QD) is a sub-micron-scale conducting device containing up to several thousand electrons. The charge transport through a quantum dot at low temperature is a quantum coherent process. Literatures [2] focuses on dots in which the electron's dynamics are chaotic or diffusive, giving rise to statistical properties that reflect the interplay between one-body chaos, quantum interference, and electron-electron interactions. The conductance through such dots displays mesoscopic fluctuations as a function of applied voltage, magnetic field, and shape deformation. In open dots, the approximation of noninteracting quasiparticles is justified, however in almost-closed dots like one of present study, where conductance occurs by tunneling, the charge on the dot is quantized, and electron-electron interactions play an important role. Transport is found to be dominated by Coulomb blockade [3], leading to peaks in the conductance that at low temperatures provide information on the dot's ground-state properties. Several statistical signatures of electron-electron interactions have been identified both theoretically and experimentally, notably in due to addition of quantum dots in the specimen. Other mesoscopic phenomena in nano composites that are affected by the charging energy include the fluctuations of the tunneling conductance and mesoscopic Coulomb blockade. [4]

3.2 Experimental.

In this work ZnS nano-cluster is dispersed in Styrofoam background to develop a system of QD array. Styrofoam- a widely used packing material popularly known as

thermocouple is prepared from the starting material styrene (vinyl benzene) by polymerization reaction. [5] Its average molecular weight is very high and its molecular formula is $(C_6H_5CHCH_2)_n$ it is a good dielectric with low physical density. The Styrofoam is dissolved in Aniline and the resulting solution is heated at 180^0 C. *In-situ* production of ZnS nano clusters is done by the passage of H_2S gas through the solution with adequate mass of Zn-acetate. The formation of ZnS nano-cluster in the dielectric background is thus followed by natural self assembly. The resulting nano-complex is caste in the form of film by spin-coating technique. The developed specimen is used for experimental investigations namely Atomic force microscopy, Optical absorption and d.c I-V characteristics. The g-V characteristics measured in the applied field direction perpendicular to the 2-D plane of the specimen.

3.3 Results and Discussions.

The ZnS nano-cluster with a size distribution in the base matrix of Styrofoam is thus prepared is used as experimental QD system. The Fig. 3.1 shows the optical absorption form UV-VIS study. The marked absorption peak corresponds to the energy 3.71 eV and is compares well with its band gap 3.67eV [6]. In fact the wide band gap of ZnS nano-clusters is clear from the study. The d.c G– V characteristics (fig. 3.2) of thin specimen at room temperature were observed by Keithley 2400 Source Meter unit and plotted by using Characterization Software. The overall nature of G–V characteristics is a marked characterization of the existence nano-cluster in the background matrix.

Following noise in mesoscopic systems [7] the observed nature of the conductance plot appeared as telegraph noise. In fact it originated from transition between two or more locally stable states. The very nature of the g fluctuation is due to the presence of QD array in the system.

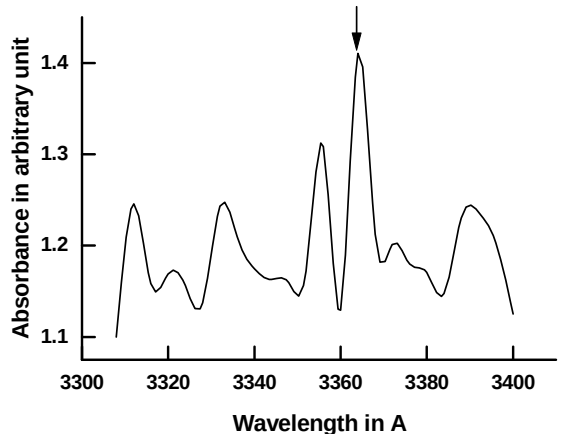

Fig 3.1: Optical absorption of the developed nano-complex at RT.

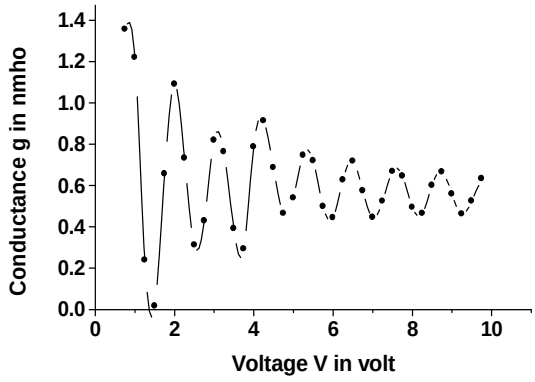

Fig 3.2: Variation of d.c conductance(G) against applied voltage. Sample dimension: thickness- 0.052 cm, area- 2.009 cm sq.

The observed conductance fluctuation is thus a fingerprint of nano-clusters in the system. In this real experimental result, the observed noise appeared as an admixture of Nyquist –Johnson, shot noise and 1/f types of noise originating mostly from the quantum confinement of 3D nano-clusters in the specimen. Apparent nature of conductance fluctuation is the indicator of formation of localized energy levels in host background. The formation of localized energy level may be attributed due to 3-D confinement of quantum dot like ionic nano-clusters within the dielectric substrate.

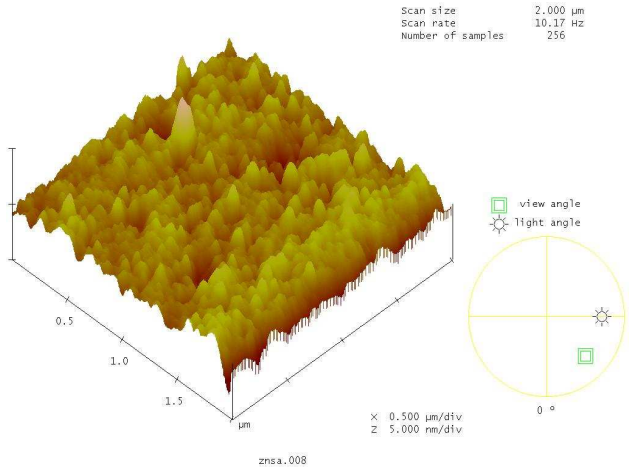

Fig 3.3: AFM microgram of ZnS nano-clusters.

The Fig. 3.3 shows the AFM picture of the developed ZnS nano clusters dispersed system. The ZnS nano cluster size in the specimen is found to vary between 70nm to 100 nm. All the measurements are carried out after six months from the preparation of sample.

3.4 Conclusions.

Formation of stable wide band gap ZnS nano clusters within polymeric substrate are distinct and clear. At RT it exhibits electrical noise like appearance as marked characteristics of nano- composite.

References.

1. T. Toyama, D. Adachi, H. Okamoto Mater. Res. Sec. Symp. Proc 2000 pp621.

2. L. Brus, P. Szajowski, W. Wilson et.al, J.Am. Chem.Soc. 117 1995 pp2915.

3. M.C. Brelle et.al., Pure Appl.Chem., 72 2000 pp101-117.

4. Y. Alhassid Rev. Mod. Phys. 72, 2000 pp895.

5 A.William Johnson, Invitation to Organic Chemistry. John and Bartlet Pub. Toronto, Canada 1999 pp652.

6. B. Bhattacharjee, D. Ganguli, K. Iakoubovskii et al Bull. Mater. Sci., 25 2002 pp175-180.

7. Yoseph Imry in Mesoscopic physics and Nanotechnology, Introduction to Mesoscopic Physics, 2/e Oxford University Press New York, 2002 pp164.

Chapter-4

Electronic Properties of Pure and Mn Doped NiO clusters.

4.1 Introduction

The research in the field of dilute magnetic semiconductor (DMS) has recently been prompted by the discovery of room-temperature ferromagnetism in transition metal (TM) doped ZnO. The field of dilute magnetic semiconductors (DMS) is currently one of the field intense activities [1]. These materials are of great interest because of the novelty of their fundamental properties and also due to their potential as the basis of future semiconductor spintronics [2].

The Nickel Oxide is known as magnetic semiconductor although its nature of magnetism in the form of present nano composite is complicated however it is known as an anti-ferromagnetic system. Transition metal oxides often exhibit novel phenomena of great fundamental and technological importance. In such cases Mn and Gd are to be the spin manipulative dopant.

The present work involves growth of NiO and Mn doped NiO as DMS materials thermal dissociation, characterization, and electrical transport studies. In following brief account of the entire work is summarized.

4.2 Experimental details

4.2.1 Sample Preparation

The Nickel acetate hydrate, analytical grade (Alpha Aesar) was heated (about 300 C) for 8h to prepare NiO powder. The developed NiO powder was grinding and strongly heated (about 350 C) for 10h. Mn doping in NiO was carried out by thermal dissociation following thermal dissociation of common acetate sol. Anhydrous Nio and Mn doped Nio were taken in form of pellets prepared by mechanical pressing at pressure 12 ton/cm^2 followed by sintering.

4.2.2 FTIR

The IR absorption of NiO powder specimen provides information about energy difference due to irrational states originating from bond bending and signature of impurities in it. The analysis was carried out in KBr window using FTIR model, IR affinity 1, Shimadzu, Japan, at high resolution.

4.2.3 UV -VIS

UV-VIS absorption spectra of the specimens were studied with model UV-2450 UV-VIS spectrophotometer, Shimadzu, Japan in the range between 190nm to 900 nm at adequate accuracy using integrating sphere attachment.

4.2.4 d.c Experiments

d.c I-V characteristics the developed pure and doped NiO specimens were studied. The developed pellet was sandwiched between two graphite electrodes for such electrical measurement. The applied field direction is perpendicular to the 2-D plane of the specimen. The d.c I-V characteristics was recorded at room temperature by Keithley 2400 (USA) Source meter unit and plotted by using characterization software.

4.3 Results and Discussions.

It has been found that NiO clusters can be developed by top-down grinding and sintering process.

FTIR analysis was carried out on pure NiO specimen (b) and on partially processed NiO specimen (a) was also carried out. Fig. 4.1 shows the FTIR spectrum of specimen (a) and (b). It shows that no substantial -COOH signature is detected curve (b). It confirms that the chemical process is complete and developed NiO specimen is pure.

d.c I-V characteristics for bulk NiO and Mn doped NiO are shown in Fig. 4.3 The nature of d.c I-V for is mostly like ohmic in nature. But due to Mn doping slopes decrease with increase in Mn concentration. The variations of d.c conductivity with Mn concentrations are shown Fig 4.4 The magnitude of conductivity decreases with in increase in Mn concentration.

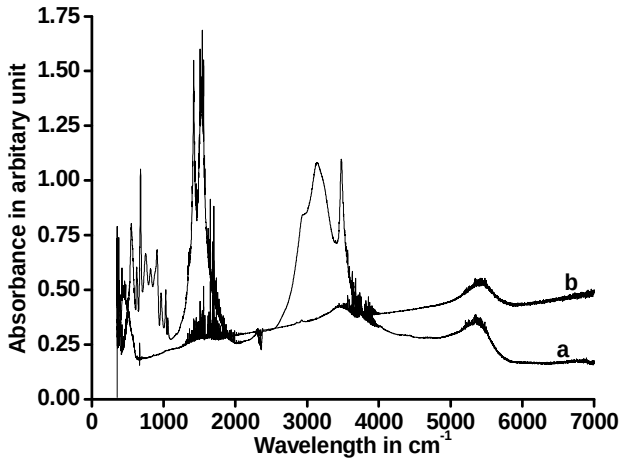

Fig. 4.1 FTIR absorption spectrum of NiO specimen (a-pure NiO,b-Mn doped NiO).

Optical absorbance of the specimen is shown Fig. 4.2. The Figure also compares the same for Mn doped NiO at mentioned Mn content. It shows that due to doping of Mn the over all nature of absorbance modified over the pure NiO variety. The estimated band gaps for specimens are found to be 3.08, 2.88, 2.76, 2.75 and 2.74eV respectively for pure (a), 3%Mn (b), 5%Mn (c), 8% Mn (d) and 10% Mn (e) concentrations. The result shows that optical band gap decrease with increase in Mn concentration however maximum effective doping level may be limited to 5% Mn concentration.

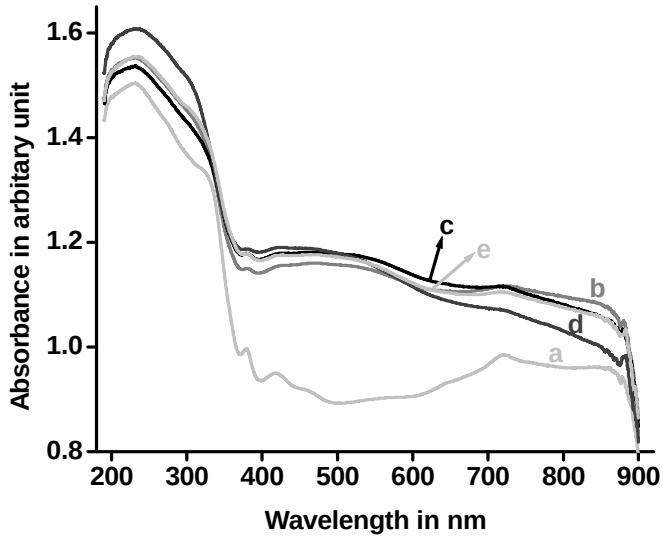

Fig. 4.2 UV-VIS absorption spectrum of Mn doped NiO.(a)Pure (b) Mn concentration 3%(c) Mn concentration 5%(d) Mn concentration 8%(e) Mn concentration 10%.

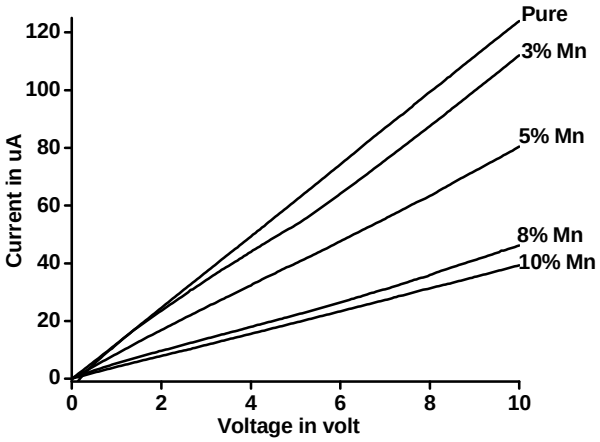

Fig. 4.3 d.c I-V characteristics for Pure and Manganese doped NiO, Average sample thickness 1mm.

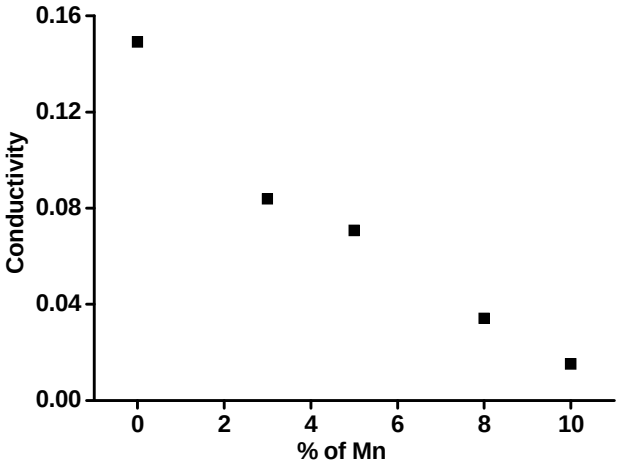

Fig: 4.4 Variation of d.c Conductivity in the unit of 10^{-5} S/cm with % of Mn Doped.

In another extension of the work variation of Magneto-resistance with applied field has been studied. The phenomena Magneto-resistance (MR) is defined as the change in electrical resistance in response to an external magnetic field (H). A brief discussion on it is given in Sec. 1.4 of Chapter 1. The formula used for calculation of the quantity is given by,

$$MR= [R(H)-R(0)] / R(0).$$

Where R(H)and R(0) are the resistance of the material in presence of applied magnetic field and zero magnetic field respectively. Figure 4.5 and 4.6 shown the variations of MR with the square of applied high and low fields.

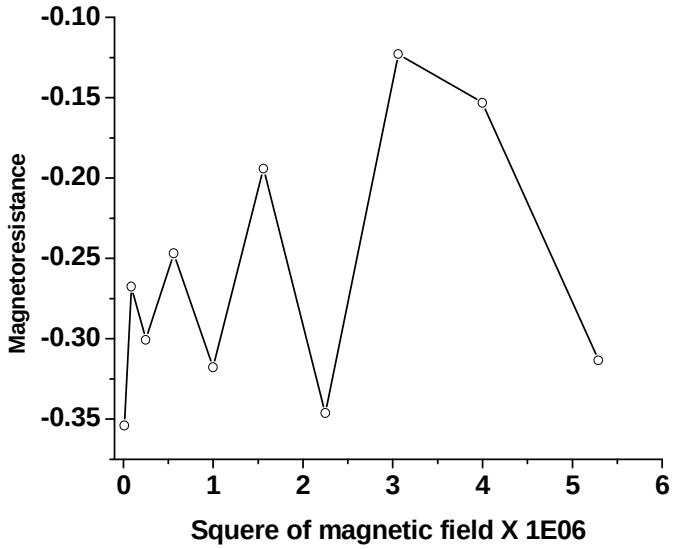

Fig.4.5: Variation of MR with squere of magnetic field in Mn (3%) doped NiO.

The negative MR is due to tunneling between continuous ferromagnetic particle along a critical path with a spin depend coulomb gap.

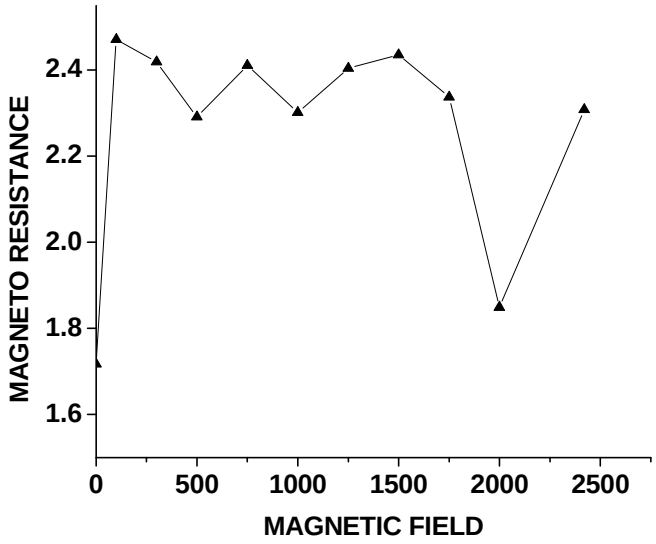

Fig.4.6: Variation of MR with magnetic field (high field) in Mn (3%) doped NiO.

4.4 Conclusions

NiO is a large band gap magnetic semiconductor. Its electrical conductivity and optical band gap can be manipulated by Mn doping in it. However the discovery of MR also opened the door to a new field of science- Spintronics (Magnetoelectronics).

References

1. F. Nasirpuri & A Nogaret Nanomagnetism and spintronics,Fabrication, Materials, Characterization and Applications- (eds), World Scientific, Singapore 2011.

2. Theory of ferromagnetic (III,Mn)V semiconductors, Jungwirth et al, Rev. Mod. Phys. 2006 78 pp809.

Chapter-5

Electrical noise in Sol-Gel synthesized ZnO nano-clusters dispersed polymer.

5.1 Introduction

The dramatic change in electrical properties of quantum sized nano-complex system over its bulk counterpart has grown considerable interest to modern science and technology. Modifications in the density of states (DOS) function with change due to quantum confinement of the system create unique electrical, optical and thermal properties. The advent of nano-sciences [1] added a new dimension over it. In an earlier study [2] authors attempted such development. Metal sulphide nano-particles have interesting optical and electrical properties [3, 4].

The present paper deals with formation of natural self-assembly of ZnO nano-clusters in dielectric substrates of synthetic polymer. These nanometer scale inclusions exhibit unique electrical properties containing quantum confinement effects and strong electrical non-linearity with apparent manifestation of electrical noise. Obtained nano-scale pattern formation yields interesting results besides controlling the size by controlling parameter of preparation.

5.2 Experimental

In this paper ZnO nano-cluster is dispersed in Styrofoam background. Styrofoam- a widely used packing material popularly known as thermocouple is prepared from the starting material styrene (vinyl benzene) by polymerization reaction. [5] The average molecular weight of Styrofoam is about 2 million and its molecular form $(C_6H_5CHCH_2)n$ it is a very good dielectric with low physical density. The Styrofoam is dissolved in chloroform and the resulting solution is heated at 80^0 C along with adequate mass of Zn- acetate. The resulting nano-complex is caste in the form of pellet by spin-coating technique. The developed specimen is used for experimental

investigations namely electrical experiment for Impedance Spectroscopy, and I – V characteristics measured in the applied field direction perpendicular to the 2-D plane.

5.3 Results and Discussions.

The zinc- oxide nano-cluster with random size variation in the base matrix of styrofoam. The particle size varies between 10nm to 100 nm.

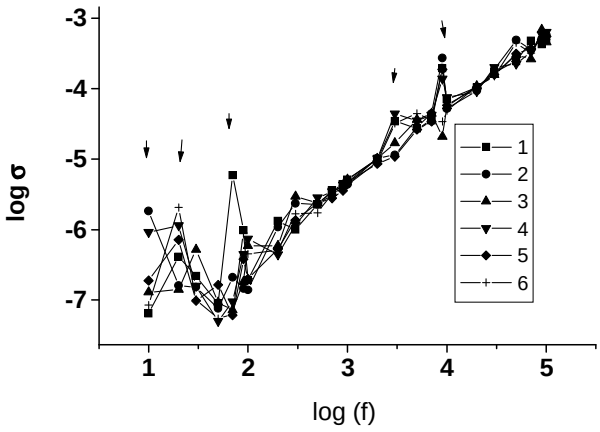

Fig. 5.1: Log conductivity plot of bulk ZnO in Styrofoam backgruond. (d=0.6 mm, C.S.A = 1.8 cm^2, p.d. = 1V). The legends corresponds to 1 to 6 represents six independent repeated measurements.

A.C conductivity measurements (Fig. 5.1) of the bulk specimen between two Copper electrodes were carried out using HIOKI 3522 LCR/Z analyzer between frequency range 10 Hz to 100 KHz.

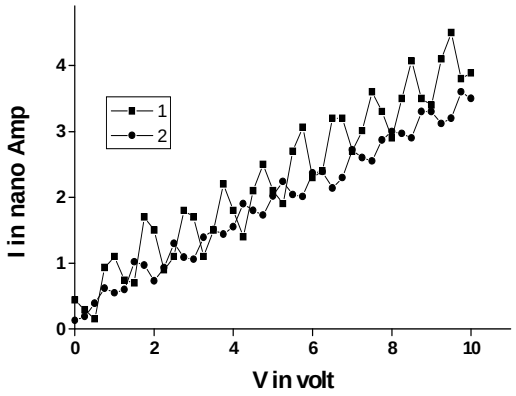

Fig.5.2: d.c I – V characteristics of thin specimen of ZnO in Styrofoam backgruond at room temperature. The legends corresponds to 1 and 2 represent six independent repeated measurements at an interval of 15 days.

Following noise in mesoscopic systems [6] the observed jumps in the conductivity plot appeared as telegraph noise. In fact it originated from transition between two or more locally stable states .A reasonable interpretation of it as due to either the motion of a scattered between two locally stable states or to the ionization or de-ionization of an impurity. The very existence of 1/f type noise is due to the presence of many activated centre in the form of nano-clusters in the specimen with smooth distribution of the barrier governing the transition between two states. The observed conductance fluctuation is thus a fingerprint or marked characteristics of the existence Nano-cluster type impurity configuration. In experimental results the observed noise appeared as an admixture of Nyquist –Johnson, shot noise and 1/f types of noise in a qualitative sense. Thus the qualitative appearance of noise is originating mostly from the quantum confinement of 3D nano-clusters in the specimen. Both fig. 5.1& 5.2 give a very clear impression that observed noise are different form typical Nyquist and or quantum noise. At RT the amplitude of fluctuation cannot be explained on the basis of thermal fluctuation of micro particles. A rigorous analysis of the observed result is under progress.

The d.c I – V characteristics (fig 5.2) of thin specimen at room temperature were observed by Keithley 2400 Source Meter unit and plotted by using Characterization Software. The overall nature of I –V characteristics is an apparent indicator of

formation of localized energy levels in host background. The formation of localized energy level may be attributed due to 3-D confinement of quantum dot like ionic nano-clusters within the dielectric substrate.

In fig. 5.2 two independent measurements are carried out at an interval of 15 days are shown. It is an interesting aspect that hyperactive nano-state did not form larger cluster to give up their nano-size characteristics. It is due to use of the dielectric Styrofoam background which provides a complete capping of the nano-clusters.

5.4 Electronic and Optical Character of Cobalt Doped Zinc Oxide.

5.4.1 Character of Cobalt doped Zinc Oxide-An Overview.

In the recent time studies on metallic oxides gained a tremendous momentum. The ultimate goal of such studies is to develop spintronic materials. Many recent studies have come up with very broad analysis on the magnetic aspect of the oxide conductors.

The research in the field of dilute magnetic semiconductor (DMS) has recently been prompted by the discovery of room-temperature ferromagnetism in transition metal (TM) doped ZnO . General consideration of using doping with 3*d* transition-metal cations in conducting oxides like SnO, semiconducting oxide ZnO or insulating oxide like TiO have been undertaken, The motivation behind these study is to realize ferromagnetism at room temperature in the systems. The results thus obtained from the studies of different worker are found conflicting. The field of dilute magnetic semiconductors (DMS) is currently one of the field intense activities. These materials are of great interest because of the novelty of their fundamental properties and also due to their potential as the basis of future semiconductor spintronic technologies which promise integration of magnetic, semiconducting and optical properties and a combination of information processing and storage functionalities.

In earlier work authors undertaken studies on pure and doped Nickel Oxide (NiO) [8] and Nickel Sulphides [9]. The overall results obtained therein are found to good. Recently Zinc Oxide (ZnO) system in both pure and doped variety are studied extensively by different worker. Pure ZnO is an eco-friendly material moreover non toxic for human bodies. ZnO NC may be useful in bio-medical applications. ZnO nano clusters are large band gap semiconductor and they can be produced by various ways [10]. It has been found that ZnO is a semiconductor with direct wide band gap 3.27 eV [11]. Studies on doped ZnO are also reported. However, the ferromagnetic aspects of the doped ZnO are found to be incomplete and conflicting.

This present work is makes an attempt to investigate various electronic and optical aspects of doped ZnO. The details of the investigation, results and analysis are given in the following subsections.

5.4.2 Experimental.

Cobalt doping in ZnO was carried out by chemical process following thermal dissociation of common acetate salt. The zinc acetate hydrate with proportionate amount of cobalt acetate, analytical grade (Alfa Aesar) were heated (about 320 C) for 8h to prepare Co doped ZnO powder. The developed Co doped ZnO powder was grinded and strongly heated (about 350 C) for 10h. Anhydrous Co doped ZnO were taken in form of pellets prepared by mechanical pressing at pressure 12 ton/cm2 followed by sintering. Two specimens with respective cobalt doping 2% (specimen-a) and 5% (specimen-b) were developed.

FTIR

The IR absorption of the Co doped ZnO powder specimen was carried out to extract information about energy difference due to vibrational [12] states originating from bond bending and signature of impurities in it. The analysis was carried out in KBr window using FTIR model, IR affinity 1, Shimadzu, Japan, at high resolution

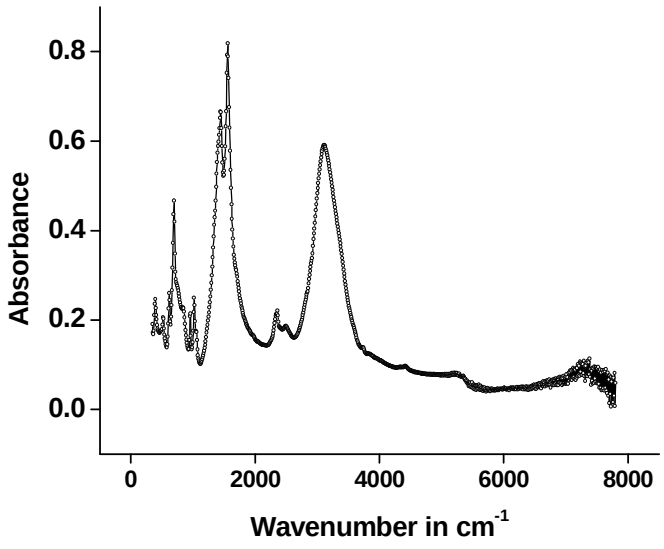

Figure5.3. FTIR absorbance of Co-doped-ZnO (Co doping level 2%)

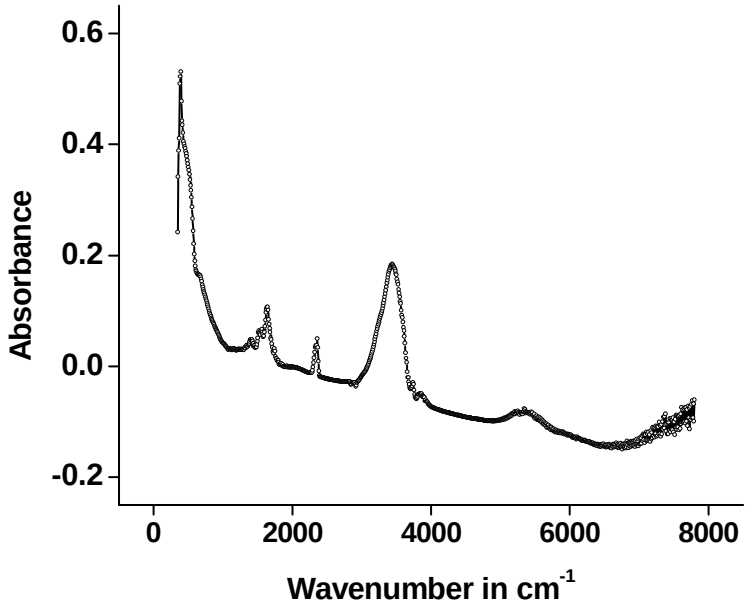

Figure5.4. FTIR absorbance of Co-doped-ZnO (Co doping level 5%).

d.c I-V Characteristics

d.c current voltage (I-V) characteristics the developed Co doped ZnO specimens were studied. The developed pellet was sandwiched between two graphite electrodes for such electrical measurement. The applied field direction is perpendicular to the 2-D plane of the specimen. The d.c I-V was recorded at room temperature 22 C by Keithley 2400 (USA) Source meter unit and plotted by using characterization software.

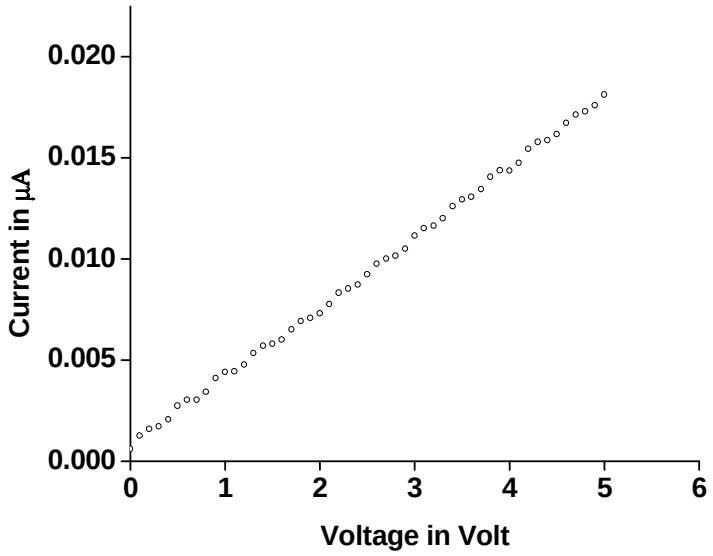

Figure 5.5. d.c I-V characteristics of Co-doped-ZnO (Co doping level 5%).

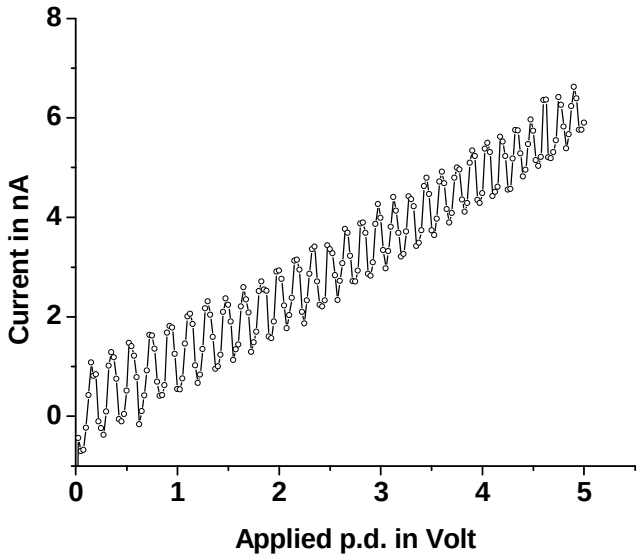

Figure5.6. d.c I-V characteristics of Co-doped-ZnO (Co doping level 2%).

UV-VIS

UV-VIS absorption spectra of the specimens were studied with model UV-2450 UV-VIS spectrophotometer, Shimadzu, Japan in the range between 190nm to 900 nm at adequate accuracy using integrating sphere attachment.

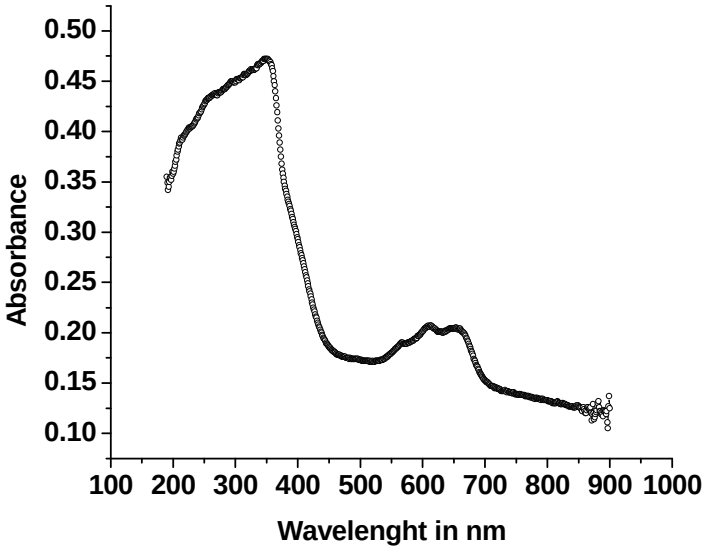

Figure5.7. Optical Absorbance Co doped ZnO (Co doping level 5%).

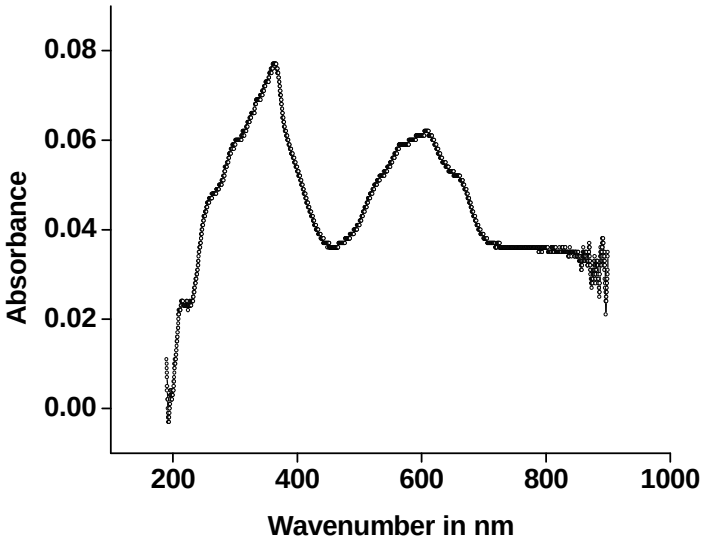

Figure5.8. Optical Absorbance Co doped ZnO (Co doping level 2%).

Magnetic measurement

Following Pal and Sarkar [13] type of magnetism in a specimen was estimated. The present technique of magnetic measurement makes use the principle if variation self inductance of a coil. The experimental specimen is placed inside the core of the coil. The arrangement when subjected to external longitudinal d.c magnetic field the self inductance of the coil changes in accordance to the magnetization of the specimen. The self inductance was measured by HIOKI (Japan) 3522 LCR Meter.

5.4.3 Results and discussion.

FTIR analysis was carried out on 2% Co doped ZnO specimen (a) and on 5% Co doped ZnO specimen (b) was also carried out. Fig. 5.3 and 5.4 show the FTIR spectrum of specimen (a) and (b) respectively. There exists no substantial -COOH signature in shown by curve (b).This confirms that the chemical process is complete and developed specimen is the desired one. The results of FTIR analysis show a clear structural difference between specimen (a) and (b).

Figures 5.5 and 5.6 show the result of d.c I-V measurement on Co doped ZnO specimens (a) and (b) respectively. The observed current exhibits oscillation like behaviour with applied voltage. It can be inferred that nano-composites do not follow Ohm's law of conduction. These functional characters of NC's are also observed in ZnO nano structures [10, 14, 15]. The existence of step like discontinuities in I – V characteristics are almost Coulomb charging like steps [16]. The thermal fluctuation effects and quantum tunneling effect appears to be competitive for these specimens. Fig.5.5 shows large amplitudes of oscillations compared to that in Fig.5.6. The change in oscillation frequency is due to difference in nano-structures, in the specimen, which is the effect of Co doping in ZnO. The 5% Co doped ZnO specimen (b) apparently exhibit lower oscillation amplitude due difference in current scale. In fact specimen (b) has greater electrical bulk conductivity than that in specimen (a) the very clear nature of I –V characteristics may be attributed due to quantum effect. The magnitudes of discontinuities are thus detectable even at near room temperature.

Optical absorbance of the specimens (a and b) is shown Fig. 5.7 and Fig.5.8 Absorption spectrum in Fig.5.7 exhibits board and valley peaks around wavelength region 340nm to 380nm. This result is the direct consequence of that the average cluster size in Co-doped ZnO specimens have a small difference due variation Co doping level. The analysis is consistent with that d.c I-V results. The band gap of Co doped ZnO was estimated from the measured optical absorbance and found to be 2.55eV and 2.85eV respectively for specimens (a) and (b). The results show that optical band decreases with increasing Co doping level.

The outcome of simple magnetic measurement shows that 5% Co doped ZnO specimen is paramagnetic (permeability $\mu \approx 1$) at room temperature. However, 2% Co doped ZnO specimen shows the signature of weak antiferromagnetic nature at RT. Both the mention systems are investigated by many workers [17-20] Tietze *et al.* [21] investigated 5% Co-doped ZnO film developed by PLD which exhibited no ferromagnetism at RT. However, it has been reported [22] that Co doped ZnO exhibit ferromagnetism at RT. Moreover there exists conflicting conclusion on analyzed magnetism of Co-doped ZnO. It may be emphasized that dilute magnetic oxides are perhaps not uniformly magnetized. The ambiguity of magnetic behavior of doped

ZnO is related to structural defects, which depend on external parameters like temperature and oxygen concentration while sample preparation.

5.5 Electronic and Optical Character of nano sized Gadolinium Doped Zinc Oxide.

5.5.1 Character of Gadolinium doped Zinc Oxide-An Overview.

Recently Zinc Oxide (ZnO) system in both pure and doped variety are studied extensively by different worker. It has been found that pure ZnO is a semiconductor with direct wide band gap 3.27 eV. [23] Studies on doped ZnO are also reported. In an earlier work [24] overall material and optical characteristics of nano sized Gadolinium oxide (Gd_2O_3) are studied. Gd_2O_3 is a semiconductor with large band gap (~4.5eV). The research in the field of dilute magnetic semiconductor (DMS) has recently been prompted by the discovery of room-temperature ferromagnetism in transition metal (TM) doped ZnO. This present work is makes an attempt to develop and investigate various electronic and optical aspects of Gd doped ZnO.

5.5.2Material Preparation

Gadolinium (Gd) doping in ZnO was carried out by chemical process following thermal dissociation of common acetate salt. Gd doping concentration was 2% and 1%. Experimental pellet was prepared using die press. The specimen diameter was 13 mm and of thickness 0.9 mm (2%) and Sample thickness-0.94mm. Area-1.362 cmsq (1%) respectively.

5.5.3 Results

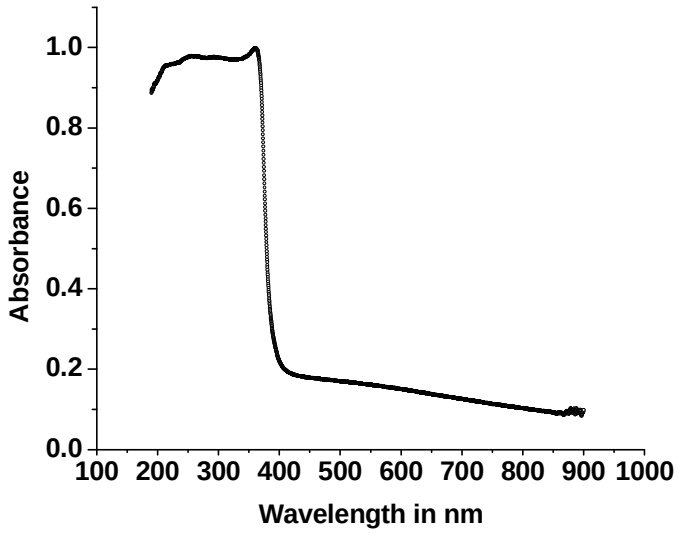

Figure5.9. Optical Absorbance of Gd doped ZnO (Gd doping level 2%).

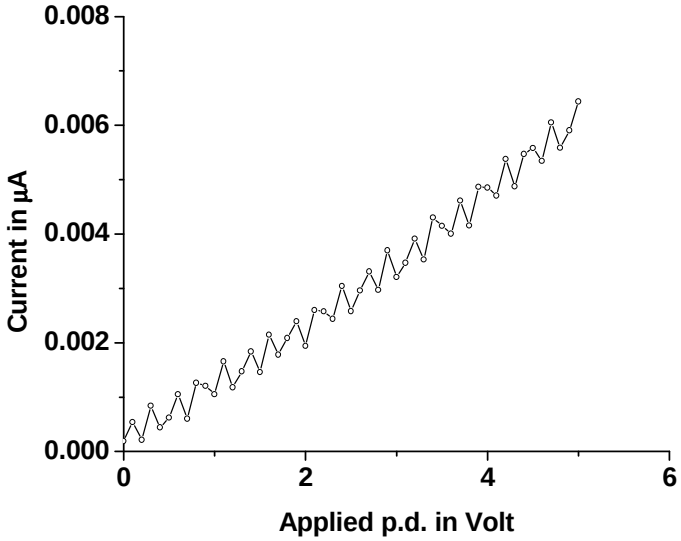

Fig.5.10 d.c I-V characteristics of Gd doped ZnO (Gd doping level 2%).

The band gap of Gd_2O_3 was estimated from the measured optical absorbance shown in fig.5.9 and found to be 3.15eV. Fig. 5.10 shows the result of d.c I-V measurement on Gd doped ZnO specimen.

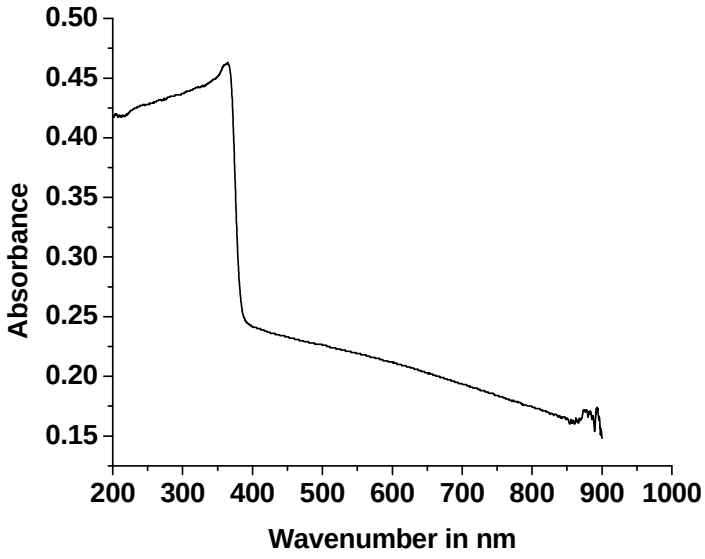

Fig.5.11. Optical Absorbance of Gd doped ZnO (Gd doping level 1%).

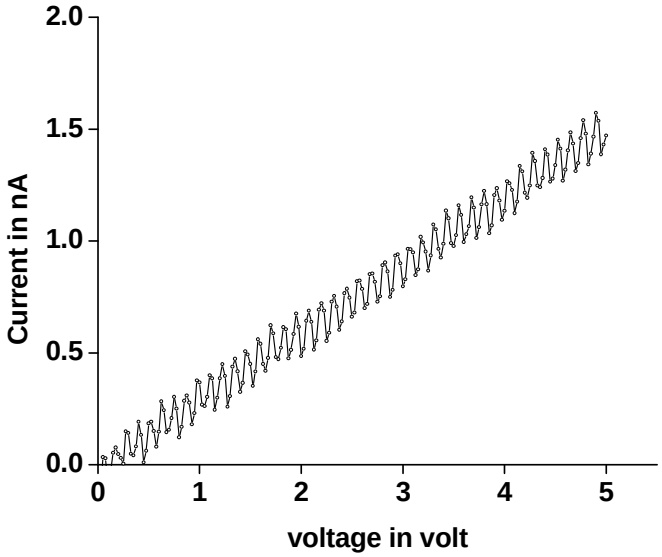

Fig.5.12 d.c I-V characteristics of Gd doped ZnO (Gd doping level 1%).

The existence of step like discontinuities in I – V characteristics are almost Coulomb charging like steps [25]. The very clear nature of I –V characteristics may be attributed due to quantum effect of developed nano-sized composite.

5.6 Conclusion

Formation of ionic nanoclusters within polymeric substrate is distinct and clear. Due to introduction of these nano-clusters enhancement of ionic conductivity is estimated to be 100 times over the pure polymer. At RT it exhibits electrical noise like appearance as marked characteristics of nano- composite. The developed nano-composite in Styrofoam base matrix is found to be stable with non degrading nano characteristics.

Formation of nano-clusters in sintered specimen is distinct and clear from I-V characteristic curve. From the study of optical absorption spectroscopy we can assume that as if three type of sized dependent nanocomposite formed and it is confirmed that Co doped ZnO nano-cluster is wide band gap semiconductor. The overall magnetic nature of the Co doped ZnO nano composite is amazing. Apart from the conflicting claim the present study finds a weak antiferromagnetism in 2% Co doped ZnO and paramagnetic nature in 5% Co doped ZnO specimen at RT. The scope of further studies on the system may provide many interesting aspect of material science.

The optical absorption data gives a direct band gap about 3.15eV which different from that of pure ZnO and pure Gd_2O_3. The developed nano material is of semiconducting nature with moderate band gap and paramagnetic in nature.

References:

1. L. Brus, P. Szajowski, W. Wilson et.al, J.Am. Chem.Soc. 1995 117 pp2915.
2. N. Gupta, H. Mallik and A. Sarkar SSP (India) 44C 2001 pp 93.
3. M.C. Brelle et.al., Pure Appl.Chem. ,2000 72, pp.101- 117.
4. N. Gupta, H. Mallik and A. Sarkar, J. Metastable and Nano Crystalline Mat. 23 2005 pp 335-338,

5 A.William Johnson, Invitation to Organic Chemistry, John and Bartlet Pub. Toronto, Canada 1999 pp652.

6. H. Mallick and A. Sarkar, Bull. Mater. Sci. 23, No 4, August 2000 pp319 – 324.

7. H. Mallik, N. Gupta and A. Sarkar, Mat. Sci. Engg C20, 2002 pp215-218.6. Yoseph Imry in Mesoscopic physics and Nanotechnology, Introduction to Mesoscopic Physics, 2/e Oxford University Press New York, 2002 pp164.

8. Moumita Barman, Somnath Paul and A. Sarkar, AIP Conf. Proc, 2013 1536, pp427.

9. Moumita Barman, Somnath Paul and A. Sarkar, Advances in Applied Science Research, 2013, 4(5), pp343-349.

10. Arnab Gangopadhyay and A. Sarkar Advances in Applied Science Research, 2011, 2 (1) pp 149-152.

11. S. J. Pearton, D. P. Norton, K. Ip, Y. W. Heo and T. Steiner, Superlatt. Microstruct, 2003 34, pp3.

12. Arup Dutta and A. Sarkar, Advances in Applied Science Research, 2011, 2 (1),pp125-128.

13. Somnath Paul and A. Sarkar, 2013,(unpublished).

14. A Gangopadhyay, Aditi Sarkar, A Sarkar, Asian J. Chem, 2011, 23, 12, pp5581-5583.

15. N. Gupta, H. Mallik and A. Sarkar, Journal of Metastable and Nanocrystalline Materials,. 2005, 23, pp 335-338.

16. S.M.Maurer et al, Phys. Rev. Lett., 1999, 83, pp1403-1406.

17. J. M. D. Coey, Jerome T. Mlack, M. Venkatesan, and P. Stamenov, IEEE Trans. on Mag, 2010**,** 46, No. 6.

18. A. Sundaresan, R. Bhargavi, N. Rangarajan, U. Siddesh and C. N. R. Rao, Phys. Rev B, 2006 74, 161306(R).

19. B. Pal and P. K.Giri, International Journal of Nanoscience, 2011**,**10, No. 1,pp1-5.

20. A. Sivagamasundari ,R. Pugaze , S. Chandrasekar , S. Rajagopan and R. Kannan, Appl Nanoscience,2013, 3,pp383–388.

21. T. Tietze *et al*.,New J. Phys., 2008, 10, p.055009..

22. A.J.Behan, A. Mokhtari, H.J. Blythe et al,.Phys. Rev. Lett, 2008, 100,47206.

23. S. J. Pearton, D. P. Norton, K. Ip, Y. W. Heo and T. Steiner, Superlatt. Microstruct. 34, 3(2003).

24. S.Paul, A.Gangopadhyay, and A.Sarkar, Advanced Materials Research Vol. 665 (2013) pp 127-131

25. N. Gupta, H. Mallik and A. Sarkar, Journal of Metastable and Nanocrystalline Materials Vol. 23 (2005) pp 335-338.

Chapter-6

Bulk and Surface Electronic Properties in synthesized CoO clusters.

6.1 Introduction

Cobalt (II) oxide (CoO) is an inorganic compound is prepared from cobalt acetated. Its appearance is a grayish black powder at RT. Its potential use lies with ceramic industry. It has been reported [1] that Cobalt oxide nanoparticle systems can be prepared by chemical sol-gel process. The capped nanoparticles of the CoO nanoparticles exhibit antiferromagnetism at low temperature. The Cobalt Oxide is a dilute magnetic semiconductor although its nature of magnetism in the form of nano composite is complicated however it is known as an anti-ferromagnetic system.

Transition metal oxides often exhibit novel phenomena of great fundamental and tecnological importance. In such cases Mn may be the spin manupulative dopant.

The present work involves growth of CoO and Mn doped CoO as DMS materials by chemical sol-gel process, studies of electrical transport. The importance and effect of transition metal doping in oxide conductor are emphasized in Sec.1.1.3 of chapter 1. In following brief account of the entire work is summarized.

6.2 Sample Preparation

The Cobalt acetate hydrate, analytical grade (Alfa Aesar) was heated (about 300 C) for 8h to prepare CoO powder (S-1). The developed CoO powder was grinding and strongly heated (about 350 C) for 10h. Mn doping in CoO was carried out by chemical sol-gel process following thermal dissociation of common acetate sol. Anhydrous CoO and Mn doped CoO were taken in form of pellets prepared by mechanical pressing at pressure 12 ton/cm^2 followed by sintering.

6.3 Experimental

d.c current voltage (I-V) characteristics the developed pure and doped CoO specimens were studied. The developed pellet was sandwiched between two graphite electrodes for such electrical measurement. The applied field direction is

perpendicular to the 2-D plane of the specimen. The d.c I-V was recorded at room temperature by Keithley 2400 (USA) Source meter unit and plotted by using characterization software. The said measurement always provides information on bulk electrical conduction. When the applied field direction is parallel to the 2-D plane, and on the specimen with suitable electrodes, the surface electrical conduction can be measured. In this work d.c bulk conductivity and d.c surface conductivity in presence of external magnetic field are measured. The later was undertaken to examine the magnetic aspects of the developed specimen.

UV-VIS absorption spectra of the Mn doped CoO specimens (3% and 10%) were studied with UV-2450 UV-VIS spectrophotometer, Shimadzu, Japan, between 190nm to900 nm at adequate accuracy using integrating sphere attachment in $BaSO_4$ background. This study is undertaken to examine it optical band in the UV-VIS region.

d.c bulk I-V characteristics for developed specimens is shown in Fig. 6.1. Fig. 6.2 shows d.c surface I-V characteristics with external magnetic field and it also compares the same to that with zero field condition. Fig. 6.3 shows the variation of optical absorbance with wavelengths in UV-VIS region.

6.4 Results and Discussions

Fig. 6.1 shows d.c bulk I-V character of pure CoO and Mn doped composite specimens. It has been analyzed that estimated conductivity, using sample geometry, increases regularly with increase in Mn concentration. Thus the effect of increasing Mn doping in CoO is leading to high conducting state in the CoO composite. The possibility enhancement of magnetic properties in the specimen may be expected to be high at higher Mn concentration.

Fig. 6.2 shows a delectable effect of external magnetic field on the theoretical conductivity in Mn doped specimen. It is an indicator of spin manipulation by inclusion of Mn in CoO at least in surface conduction mode.

The UV-VIS absorption spectra of sample A (3%Mn) and sample B (10%Mn) is shown in the fig. 6.3. The absorption peak for the second sample is blue shifted by $\Delta\lambda$=18.92777nm with respect to first sample. The blue shift is due to quantum size

effect which also indicates the presence of nano sized Mn_2O_3 particles with shorter dimension [4,5].

The indirect band gap of Mn doped CoO was estimated from the measured optical absorbance shown in Fig. 6.3 and found to be 2.43eV and 2.39.eV respectively for 3% and 10% Mn doped specimens.

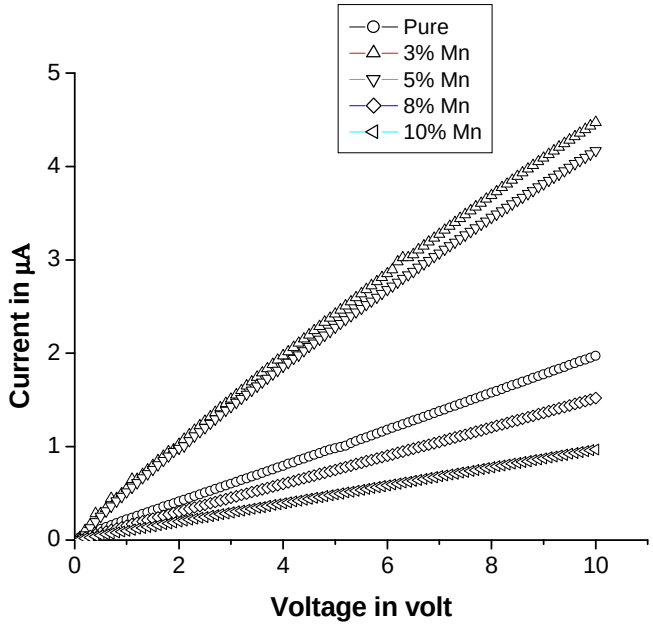

Fig. 6.1 d.c bulk I-V characteristics of Pure and Mn doped CoO.

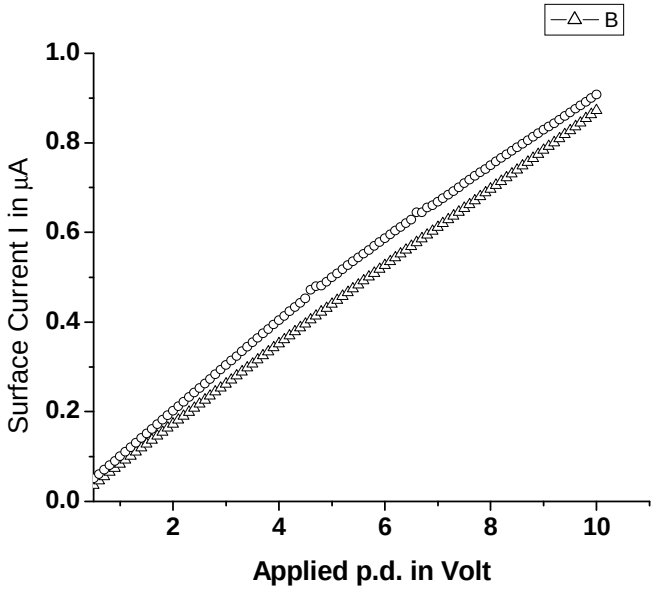

Fig. 6.2: d.c surface I-V characteristics of the developed material with 5% Mn doped CoO at external Magnetic field 500 G (upper Curve) and at Zero field (Lower Curve).

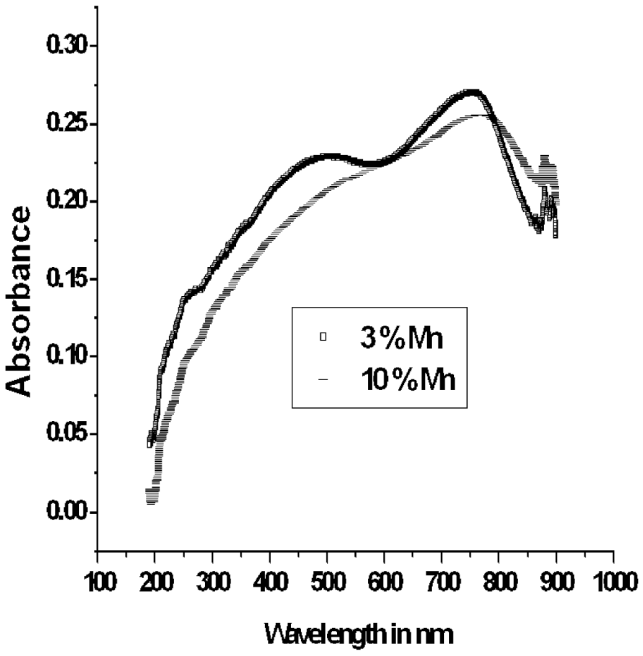

Fig. 6.3 UV-VIS absorbance spectra for Mn doped CoO.

.

6.5 Other doped oxides

In order to make the more exhaustive Titanium and Nickel doped CoO were developed and studied in this work. Titanium oxide (TiO) is an insulator with no remarkable magnetism in it. However, role Titanium doping in field of DMS has been mentioned Sec 1.4 in chapter 1. On the other hand Nickel oxide (NiO) is an insulator with anti ferromagnetic property at RT. In fact NiO is a true DMS at RT.

In this work both Titanium (Ti) doped CoO and Nickel (Ni) doped CoO were developed following chemical route discussed in sec.6.2 . The experimental specimens and experiments on them were carried out following the same procedure as discussed in sec.6.2 and sec.6.3.

6.5.1 Results and discussions

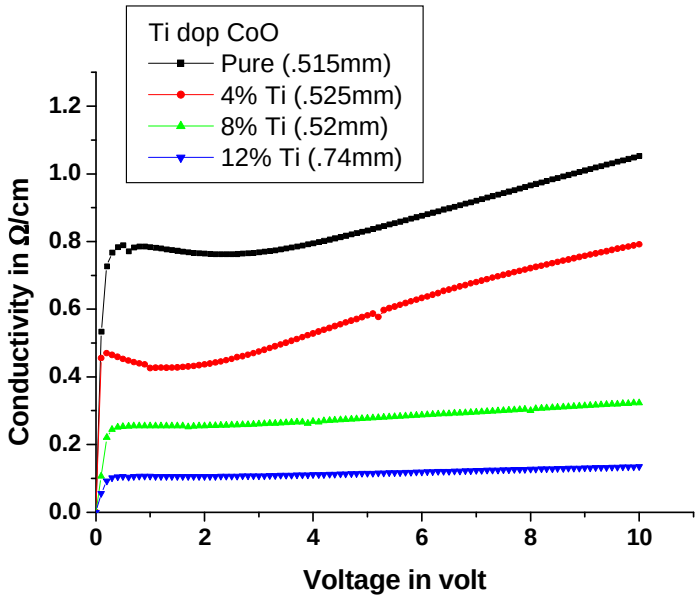

Fig. 6.4 d.c bulk I-V characteristics of Pure and Ti doped CoO.

Figure 6.4 shows the results of d.c I-V characteristics of Ti doped CoO at different Ti doping level and also compares the same to that of pure CoO. It also shows that increase in Ti doping level CoO system becomes to have more and more insulating property.

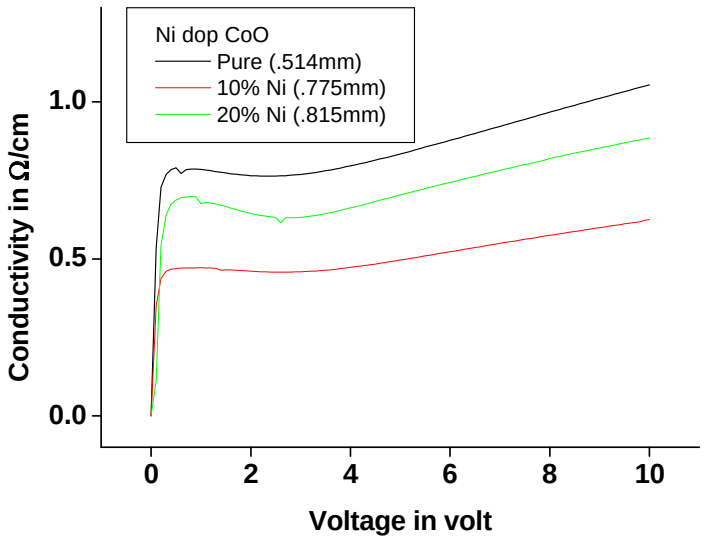

Fig. 6.5 d.c bulk I-V characteristics of Pure and Ni doped CoO.

Figure 6.5 shows the results of d.c I-V characteristics of NiO doped CoO at different Ni doping level and also compares the same to that of pure CoO. It also shows that increase in Ni doping level CoO system becomes to have more and more insulating property like that in Ti doped CoO.

6.6 Conclusion

CoO is magnetic semiconductor with moderate band gap by varying the size of the nano-particles size and doping its electronic properties can be tailored. Mn could be good dopant in CoO system for manipulation of magnetic properties it. Ti and Ni doped CoO are not suitable for DMS application however they might be important as wide band semiconductors for other applications.

References

1. A. Tomou et al , J. Appl. Phys. 2006, 99, 123915.
2. Nanomagnetism and spintronics ,Fabrication, Materials, Characterization and Applications- F.Nasirpuri & A Nogaret (eds), World Scientific, Singapore,2011.
3. Theory of ferromagnetic (III,Mn)V semiconductors, Jungwirth et al, Rev. Mod. Phys. 2006 78 pp809.
4. Y. Kayanuma, Phys. Rev. B 1998, 85 pp9797.
5. L. Brus, J. Phys. Chem. 1986, 90 pp2555.

OVERALL CONCLUSION

Formation of ionic nano-clusters NiS within polymeric substrate is distinct and clear from I-V characteristic curve. From the study of optical absorption spectroscopy we can assume that as if three type of sized dependent nano-composite formed and it is confirmed that NiS nano-cluster is a small band gap semiconductor. The overall magnetic nature of the NiS nano composite is amazing. Apart conflicting claim the present study finds a weak ferromagnetism below 40 K and paramagnetic above it in the developed NiS specimen. The scope of further studies on the system may provide many interesting aspect of material science. NiS nano particles can harvest in energy from both sunlight and the earth's heat radiation with higher efficiency than conventional solar cell. The developed NiS composite successfully exhibits the mentioned property. The overall IR absorbance of the developed NiS complex is observed to be good and encouraging.

Formation of stable wide band gap ZnS nano clusters within polymeric substrate are distinct and clear. At RT it exhibits electrical noise like appearance as marked characteristics of nano- composite.

NiO is a large band gap magnetic semiconductor. Its electrical conductivity and optical band gap can be tailored by Mn doping in it.

Formation of ionic ZnO nanoclusters within polymeric substrate is distinct and clear. Due to introduction of these nano-clusters enhancement of ionic conductivity is estimated to be 100 times over the pure polymer host. At RT it exhibits electrical noise like appearance as marked characteristics of nano- composite. The developed nano-composite in Styrofoam base matrix is found to be stable with non degrading nano characteristics.

Formation of nano-clusters of Co doped ZnO in sintered specimen is distinct and clear from I-V characteristic curve. From the study of optical absorption spectroscopy we can assume that as if three type of sized dependent nanocomposite formed and it is confirmed that Co doped ZnO nano-cluster is wide band gap semiconductor. The overall magnetic nature of the Co doped ZnO nano composite is amazing. Apart from

the conflicting claim the present study finds a weak antiferromagnetism in 2% Co doped ZnO and paramagnetic nature in 5% Co doped ZnO specimen at RT. The scope of further studies on the system may provide many interesting aspect of material science.

Formation of nano-clusters in the Gd doped ZnO specimen is distinct and clear from I-V characteristic curve. The optical absorption data gives a direct band gap about 3.15eV which different from that of pure ZnO and pure Gd_2O_3. The developed nano material is of semiconducting nature with moderate band gap and paramagnetic in nature.

CoO is magnetic semiconductor with wide band gap. By varying the size of the nano-particles size and doping its electronic properties can be tailored. Mn could be good dopant in CoO system for manipulation of magnetic properties it. Ti and Ni doped CoO are not suitable for DMS application however they might be important as wide band semiconductors for other applications.